ANL-78-51

A NODAL METHOD FOR SOLVING TRANSIENT FEWGROUP NEUTRON DIFFUSION EQUATIONS

by

R. A. Shober

BASE TECHNOLOGY

U of C-AUA-USDOE

ARGONNE NATIONAL LABORATORY, ARGONNE, ILLINOIS

Prepared for the U. S. DEPARTMENT OF ENERGY
under Contract W-31-109-Eng-38

Printed in the United States of America
Available from
National Technical Information Service
U. S. Department of Commerce
5285 Port Royal Road
Springfield, Virginia 22161
Price: Printed Copy $6.00; Microfiche $3.00

Distribution Category:
LMFBR Physics (UC-79d)

ANL-78-51

ARGONNE NATIONAL LABORATORY
9700 South Cass Avenue
Argonne, Illinois 60439

A NODAL METHOD FOR SOLVING TRANSIENT FEWGROUP NEUTRON DIFFUSION EQUATIONS

by

R. A. Shober

Applied Physics Division

June 1978

TABLE OF CONTENTS

LIST OF TABLES

LIST OF FIGURES

A Nodal Method for Solving Transient Fewgroup Neutron Diffusion Equations

by

R. A. Shober
Argonne National Laboratory

ABSTRACT

A nodal method for multidimensional light water reactor (LWR) static and transient analysis is presented in this report. This method efficiently solves one- or two-group diffusion equations using an analytic solution procedure. This report details significant improvements made to those aspects of the method previously reported in the literature. Eigenvalues and power distributions are presented for several static benchmark problems. Time-dependent results for a difficult two-dimensional BWR kinetics benchmark problem are presented. A reference solution for this benchmark problem is also presented. The results presented in this report are summarized, and suggestions are made as to appropriate ways to extend this work to multigroup fast breeder reactor analysis.

I. INTRODUCTION

In this report, a method for solving the multidimensional, one- or two-group time-dependent neutron diffusion equations is developed. Although the specific method discussed here is limited to one or two neutron groups, the techniques used in the development of the method are important for an understanding of future methods development work which will be carried out in order to solve the multigroup neutron diffusion equations.

For light water reactors (LWR's), the time dependent one- or two-group diffusion equations have proven to be a reliable tool for analyzing reactor accidents. After appropriate fuel assembly homogenization procedures[1] have been performed, the analysis of an LWR involves the solution of a diffusion problem over a series of large, homogeneous regions; generally as large as 20 cm on a side. To obtain accurate solutions to this problem using finite difference methods, many spatial mesh points are often used. In general, the number of mesh points required in any one dimension to obtain accurate finite difference results is proportional to the number of neutron diffusion lengths present in that dimension of the reactor. The neutron diffusion length for group g neutrons is defined as[2]

$$L_g = \sqrt{\frac{D_g}{\Sigma_{a_g}}} \tag{I.1}$$

The diffusion length for thermal neutrons in an LWR can be as small as 2.5 cm for some cases. Therefore, due to the large number of unknowns in each dimension, a multidimensional analysis of an LWR using finite difference methods can be very expensive.

In the last few years, considerable success has been obtained in developing so-called nodal methods for solving multidimensional LWR diffusion problems. For many years, nodal methods comprised a variety of schemes for solving the diffusion equations in which a set of "coupling coefficients" were defined which relate the fluxes in two adjacent regions to the current at the interface between the regions. These "coupling coefficients" were often evaluated from fine-mesh calculations and then used for a variety of reactor conditions. Although the coefficients may give acceptable results for one reactor configuration, it is dangerous to extend their use very far beyond the original reactor configuration used to calculate them. The nodal schemes which have been developed recently, however, differ from the above methods in that the "coupling coefficients" are rigorously defined in some way.[3,4,5,7,8,9] The methods also differ in that some of them[3,5] use the partial neutron currents as the final unknowns for which a solution is required. However, the common thread among all of the above schemes is that polynomial expansions are used to solve the diffusion equation on a local basis (within each region), and these solutions are used to define the coupling between one unknown and another. In fact, this same definition includes finite element methods.[6] As Werner has pointed out,[4] the newly developed nodal schemes are variations on the finite element method in which the weight functions are defined in ways other than the conventional Galerkin scheme.

In Chapters II and III, the development of a nodal scheme for solving multidimensional, time-dependent one- or two-group neutron diffusion equations is reviewed. This method has been previously reported in the literature[7,8,9]. This report documents the following:

a) An improved time dependent strategy which reduces the computing time spent re-calculating the coefficient matrices.

b) A new representation of the transverse leakage term which yields significant improvement in spatial accuracy.

c) A reference solution to Benchmark Problem 14-A1,[10] as well as coarse mesh solutions from the methods developed here.

The development of the method in one spatial dimension is shown in Chapter II. The extension of the method to two-dimensional time dependent problems is shown in Chapter III. The results of several benchmark problems are given in Chapter IV. Conclusions based on the above benchmark problems, and recommendations for future study are presented in Chapter V.

II. DEVELOPMENT IN ONE DIMENSION

A. Introduction

In this Chapter, methods for solving the one-dimensional diffusion equation are discussed. The static diffusion equation is integrated over each homogeneous region to yield the integrated nodal equation. To solve this equation, auxiliary relationships between the fluxes and currents are necessary. These relationships can be derived in various ways. Two derivations are discussed in this Chapter; the first based on response matrices, the second based on an analytic solution to the diffusion equation over each homogeneous region. It is shown that the analytic solution technique is simply a special case of the more general response matrix method. Finally, a technique for solving the one-dimensional, time-dependent diffusion equation is described.

B. The One-Dimensional Diffusion Equation

The one-dimensional, time-independent diffusion equation is

$$-\frac{d}{dx}[D(x)]\frac{d}{dx}[\phi(x)] + [\Sigma_T(x)]\,[\phi(x)]$$

$$= \frac{1}{\lambda}[\chi]\,[\nu\Sigma_f(x)]^T\,[\phi(x)] \qquad \text{(II.1)}$$

where

$[D(x)]$	is a diagonal G×G matrix consisting of the diffusion coefficients
$[\phi(x)]$	is a column vector of length G consisting of the neutron fluxes
$[\Sigma_T(x)]$	is a G×G matrix consisting of the absorption and scattering cross sections
$[\chi]$	is a column vector of length G consisting of the fission spectrum
$[\nu\Sigma_f(x)]$	is a column vector of length G consisting of nu times the fission cross section
G	is the number of neutron energy groups.

The one-dimensional reactor configuration R = [0,X] is divided into a partition π: $0<x_1, \ldots <x_I = X$, with the restriction that any region

$$x_i \leq x \leq x_{i+1}$$

be homogeneous. Eq. (II.1) is then integrated over $x_i \leq x \leq x_{i+1}$:

$$[J(x_{i+1})] - [J(x_i)] + h_i\ [\Sigma_{T_i}]\ [\bar{\phi}_i]$$

$$= \frac{1}{\lambda} h_i\ [\chi]\ [\nu\Sigma_{f_i}]^T\ [\bar{\phi}_i] \qquad \text{(II.2)}$$

where

$$[J(x_i)] = -\ [D_i] \frac{d}{dx} [\phi(x)] \bigg|_{x=x_i}$$

$$[\bar{\phi}_i] = \frac{1}{h_i} \int_{x_i}^{x_{i+1}} [\phi(x)]\ dx$$

$$[\Sigma_{T_i}] = [\Sigma_T(x)] \bigg|_{x\ \epsilon\ R_i}$$

$$R_i = (x_i,\ x_{i+1})$$

$$h_i = x_{i+1} - x_i$$

Equation (II.2) shows that the average fluxes in adjacent regions are dependent on the net currents at the interface between two regions. Therefore, it is desired to obtain a relationship between the average fluxes $[\phi_{i-1}]$ and $[\phi_i]$ and the current at x_i, $[J(x_i)]$.

C. Derivation Based on Response Matrices

Let us define J^+_{gi} and J^-_{gi} as the partial currents in the +x and -x directions at x_i. The corresponding G-element column vectors of group partial currents are therefore $[J^+_i]$ and $[J^-_i]$. Then for region R_i in a vacuum, the transmission matrices $[T^{\pm}_i]$ are defined as

$$[T_i^+]\ [J_i^+] = [J_{i+1}^+]$$
$$[T_i^-]\ [J_i^-] = [J_{i-1}^-] \qquad \text{(II.3)}$$

These results can be generalized such that they are defined over an arbitrary distance between x_i and x_{i+1} (or x_i and x_{i-1}). Let x be any point in the interval $[x_{i-1}, x_{i+1}]$. Then Eqs. (II.3) above become

$$[T^+(x)]\ [J_i^+] = [J^+(x)] \text{ for } x_i \leq x \leq x_{i+1}$$
$$[T^-(x)]\ [J_i^-] = [J^-(x)] \text{ for } x_{i-1} \leq x \leq x_i \qquad \text{(II.4)}$$

The reflection matrices $[R_i^{\pm}]$ are defined as

$$[R_i^+]\ [J_i^+] = [J_i^-]$$
$$[R_i^-]\ [J_i^-] = [J_i^+] \qquad \text{(II.5)}$$

In the general scheme, Eqs. (II.5) become

$$[R^+(x)]\ [J_i^+] = [J_i^-] \text{ for } x_i \leq x \leq x_{i+1}$$
$$[R^-(x)]\ [J_i^-] = [J_i^+] \text{ for } x_{i-1} \leq x \leq x_i \qquad \text{(II.6)}$$

In Eqs. (II.4) and (II.6) above, the point x represents the location of the point x_{i+1} or x_{i-1}; whichever is applicable.

For R_i imbedded in the reactor, the following matrix equation can be derived:

$$\begin{bmatrix} [J_i^+] \\ [J_i^-] \end{bmatrix} = [R(x)] \begin{bmatrix} [J^+(x)] \\ [J^-(x)] \end{bmatrix} \qquad \text{(II.7)}$$

for $x_i \leq x \leq x_{i+1}$. The matrix $[R(x)]$ can be shown to be

$$[R(x)] = \begin{bmatrix} [T^+(x)]^{-1} & -[T^+(x)]^{-1}\ [R^-(x)] \\ \\ [R^+(x)]\ [T^+(x)]^{-1} & \begin{matrix} -[R^+(x)][T^+(x)]^{-1}\ [R^-(x)] \\ +[T^-(x)] \end{matrix} \end{bmatrix} \tag{II.8}$$

Equations (II.7, 8) show that a relationship exists between the partial currents at x_i and the partial currents at x which depend only on the material properties in the region (x_i, x).

A P-1 expansion of the angular flux at point x_i gives the following relationship:

$$\begin{bmatrix} [\phi_i] \\ [J_i] \end{bmatrix} = \begin{bmatrix} 2[I] & 2[I] \\ [I] & -[I] \end{bmatrix} \cdot \begin{bmatrix} [J_i^+] \\ [J_i^-] \end{bmatrix} \tag{II.9}$$

Therefore, Eq. (II.7) becomes

$$\begin{bmatrix} [\phi_i] \\ \\ [J_i] \end{bmatrix} = \begin{bmatrix} 2[I] & 2[I] \\ \\ [I] & -[I] \end{bmatrix} [R(x)] \begin{bmatrix} \frac{1}{4}[I] & \frac{1}{2}[I] \\ \\ \frac{1}{4}[I] & -\frac{1}{2}[I] \end{bmatrix} \begin{bmatrix} [\phi(x)] \\ \\ [J(x)] \end{bmatrix} \tag{II.10}$$

for $x_i \leq x \leq x_{i+1}$. Let us re-write Eq. (II.10) as

$$\begin{bmatrix} [\phi_i] \\ \\ [J_i] \end{bmatrix} = [S(x)] \begin{bmatrix} [\phi(x)] \\ \\ [J(x)] \end{bmatrix} \tag{II.11}$$

Equation (II.11) is then multiplied by $[S(x)]^{-1}$. Assuming that the inverse exists, we have

$$[S(x)]^{-1} \begin{bmatrix} [\phi_i] \\ [J_i] \end{bmatrix} = \begin{bmatrix} [\phi(x)] \\ [J(x)] \end{bmatrix} \tag{II.12}$$

If Eq. (II.12) is integrated from x_i to x_{i+1}, the following equation is obtained

$$[U_i] \begin{bmatrix} [\phi_i] \\ [J_i] \end{bmatrix} = h_i \begin{bmatrix} [\bar{\phi}_i] \\ [\bar{J}_i] \end{bmatrix} \tag{II.13}$$

where

$$h_i \begin{bmatrix} [\bar{\phi}_i] \\ [\bar{J}_i] \end{bmatrix} = \int_{x_i}^{x_{i+1}} \begin{bmatrix} [\phi(x)] \\ [J(x)] \end{bmatrix} dx$$

$$[U_i] = \int_{x_i}^{x_{i+1}} [S(x)]^{-1} \, dx$$

Equation (II.13) defines a relationship between the average properties in (x_i, x_{i+1}) to the values present at point x_i. To obtain a similar relationship between the properties at x_i and the average properties over (x_{i-1}, x_i), we return to Eq. (II.11) with a change in subscripts:

$$\begin{bmatrix} [\phi_{i-1}] \\ [J_{i-1}] \end{bmatrix} = [S(x)] \begin{bmatrix} [\phi(x)] \\ [J(x)] \end{bmatrix} \tag{II.14}$$

where $x_{i-1} \leq x \leq x_i$. Denoting

$$[S(h_{i-1})] = [S(x)] \Big|_{x=x_i}$$

we find that Eq. (II.14) becomes

$$[S(x)]^{-1} [S(h_{i-1})] \begin{bmatrix} [\phi_i] \\ [J_i] \end{bmatrix} = \begin{bmatrix} [\phi(x)] \\ [J(x)] \end{bmatrix} \tag{II.15}$$

If then Eq. (II.15) is integrated from x_{i-1} to x_i, we obtain:

$$[W_{i-1}] \begin{bmatrix} [\phi_i] \\ [J_i] \end{bmatrix} = h_{i-1} \begin{bmatrix} [\bar{\phi}_{i-1}] \\ [\bar{J}_{i-1}] \end{bmatrix} \tag{II.16}$$

where

$$[W_{i-1}] = \int_{x_{i-1}}^{x_i} [S(x)]^{-1} \, dx \, [S(h_{i-1})]$$

Let us rewrite Eqs. (II.13) and (II.16)

$$[U_i] \begin{bmatrix} [\phi_i] \\ [J_i] \end{bmatrix} = h_i \begin{bmatrix} [\bar{\phi}_i] \\ [\bar{J}_i] \end{bmatrix} \tag{II.13}$$

$$[W_{i-1}] \begin{bmatrix} [\phi_i] \\ [J_i] \end{bmatrix} = h_{i-1} \begin{bmatrix} [\bar{\phi}_{i-1}] \\ [\bar{J}_{i-1}] \end{bmatrix} \tag{II.16}$$

Each Eq. (II.13) or (II.16) represents 2G equations. Let us write only the top G equations in the following way:

$$[U_i^{1,1}] \, [\phi_i] + [U_i^{1,2}] \, [J_i] = h_i \, [\bar{\phi}_i] \tag{II.17}$$

$$[W_{i-1}^{1,1}] \, [\phi_i] + [W_{i-1}^{1,2}] \, [J_i] = h_{i-1} \, [\bar{\phi}_{i-1}] \tag{II.18}$$

Multiplying (II.17) by $[U_i^{1,1}]^{-1}$ and (II.18) by $[W_{i-1}^{1,1}]^{-1}$ (assuming the inverses exist), we obtain

$$[\phi_i] + [U_i^{1,1}]^{-1} \, [U_i^{1,2}] \, [J_i] = h_i \, [U_i^{1,1}]^{-1} \, [\bar{\phi}_i]$$

$$[\phi_i] + [W_{i-1}^{1,1}]^{-1} \, [W_{i-1}^{1,2}] \, [J_i] = h_{i-1} \, [W_{i-1}^{1,1}]^{-1} \, [\bar{\phi}_{i-1}]$$

Subtracting the above two equations gives

$$[U_i^{1,1}]^{-1}\ [U_i^{1,2}]\ [J_i] - [W_{i-1}^{1,1}]^{-1}\ [W_{i-1}^{1,2}]\ [J_i]$$

$$= h_i\ [U_i^{1,1}]^{-1}\ [\bar{\phi}_i] - h_{i-1}\ [W_{i-1}^{1,1}]^{-1}\ [\bar{\phi}_{i-1}]$$

or

$$[J_i] = \left\{[U_i^{1,1}]^{-1}\ [U_i^{1,2}] - [W_{i-1}^{1,1}]^{-1}\ [W_{i-1}^{1,2}]\right\}^{-1}$$

$$\cdot \left\{h_i\ [U_i^{1,1}]^{-1}\ [\bar{\phi}_i] - h_{i-1}\ [W_{i-1}^{1,1}]^{-1}\ [\bar{\phi}_{i-1}]\right\} \tag{II.19}$$

Equation (II.19) shows that a relationship exists between the current $[J_i]$ and the adjacent average fluxes $[\bar{\phi}_{i-1}]$ and $[\bar{\phi}_i]$. This relationship involves only the material properties in these adjacent regions. The only additional assumptions made in this derivation were that a P-1 expansion was made at the interface (diffusion theory is valid at that point), and that the necessary inverses exist. Therefore, the response matrices could be evaluated in any conventional manner, and the global problem solved within a nodal framework.

D. Derivation Based on Analytic Solutions to the Diffusion Equation

In this Section, analytic solutions to the diffusion equation will be used to derive the coupling relationship between neighboring regions. Let us first write Eq. (II.1) in P-1 form:

$$\frac{d}{dx}\ [J(x)] + [\textstyle\sum_T(x)]\ [\phi(x)] = \frac{1}{\lambda}\ [\chi]\ [\nu\textstyle\sum_f(x)]^T\ [\phi(x)] \tag{II.20}$$

$$\frac{d}{dx}\ [\phi(x)] + [D(x)]^{-1}\ [J(x)] = 0$$

and let us further define

$$[\Phi(x)] = \text{col}\ \left\{[\phi(x)],\ [J(x)]\right\} \tag{II.21a}$$

$$[N(x)] = \begin{bmatrix} [0] & [D(x)]^{-1} \\ [\Sigma_T(x)] - \frac{1}{\lambda}[\chi]\,[\nu\Sigma_f(x)]^T & [0] \end{bmatrix} \tag{II.21b}$$

Therefore Eqs. (II.20) can be written as:

$$\frac{d}{dx}[\Phi(x)] + [N(x)]\,[\Phi(x)] = 0 \tag{II.22}$$

This equation can be solved analytically over a homogeneous region R_i to give:

$$[\Phi(x)] = e^{-[N_i]\,(x-x_i)}\,[\Phi(x_i)] \tag{II.23}$$

Integrating (II.23) from x_i to x_{i+1}, dividing by h_i, and rearranging yields:

$$[N_i]\,h_i\,[\bar{\Phi}_i] = \left[[I] - e^{-[N_i]\,h_i}\right][\Phi(x_i)] \tag{II.24}$$

where

$$[\bar{\Phi}_i] = \frac{1}{h_i}\int_{x_i}^{x_{i+1}} [\Phi(x)]\,dx$$

and $[N_i]$ is the matrix $[N(x)]$ for $x \in R_i$.

Similarly, we can integrate Eq. (II.23) in the negative direction over homogeneous region R_{i-1} to obtain

$$-[N_{i-1}]\,h_{i-1}\,[\bar{\Phi}_{i-1}] = \left[[I]-e^{[N_{i-1}]\,h_{i-1}}\right][\Phi(x_i)] \tag{II.25}$$

Comparing Eqs. (II.13) and (II.16) to Eqs. (II.24) and (II.25), we observe that

$$[U_i] = [N_i]^{-1}\left[[I] - e^{-[N_i]h_i}\right] \tag{II.26a}$$

$$[W_{i-1}] = -[N_{i-1}]^{-1}\left[[I] - e^{[N_{i-1}]h_{i-1}}\right] \tag{II.26b}$$

Therefore, the matrices $[U_i]$ and $[W_{i-1}]$ are made up solely of cross sections and mesh lengths of regions R_i and R_{i-1}, respectively.

To continue the development, the following trigonometric identities are recalled:

$$1-e^{-x} = 1 - \cosh x + \sinh x$$

$$1-e^{x} = 1 - \cosh x - \sinh x$$

Substituting these relationships into Eqs. (II.24) and (II.25), adding the resulting equations together, and rearranging gives:

$$(\sinh^{-1}[N_i]h_i)\left\{[I] - \cosh[N_i]h_i\right\}[\Phi(x_i)]$$

$$+ [\Phi(x_i)] = (\sinh^{-1}[N_i]h_i)[N_i]h_i[\bar{\Phi}_i] \tag{II.27a}$$

$$(\sinh^{-1}[N_{i-1}]h_i)\left\{[I] - \cosh[N_{i-1}]h_{i-1}\right\}[\Phi(x_i)]$$

$$- [\Phi(x_i)] = -(\sinh^{-1}[N_{i-1}]h_{i-1})[N_{i-1}]h_{i-1}[\bar{\Phi}_{i-1}] \tag{II.27b}$$

Now recall the additional trigonometric relationship

$$(\sinh^{-1}x)(1-\cosh x) = -\tanh\frac{x}{2}$$

Adding Eqs. (II.27) together, and using the above relationship yields:

$$-(\tanh[N_i]h_i/2 + \tanh[N_{i-1}]h_{i-1}/2)[\Phi(x_i)]$$

$$= (\sinh^{-1}[N_i]\,h_i)\,[N_i]\,h_i\,[\bar{\Phi}_i] \qquad \text{(II.28)}$$

$$-(\sinh^{-1}[N_{i-1}]\,h_{i-1})\,[N_{i-1}]\,h_{i-1}\,[\bar{\Phi}_{i-1}]$$

Let us now define

$$[A^i] = (\tanh[N_i]\,h_i/2)$$

$$[B^i] = (\sinh^{-1}[N_i]\,h_i)\,[N_i]\,h_i \qquad \text{(II.29)}$$

We note that Eq. (II.28) represents 2G equations; therefore the matrices $[A^i]$ and $[B^i]$ are 2G × 2G matrices. Let us denote these matrices as being composed of four blocks, each block being a G × G matrix. We observe, based on the definition Eq. (II.29), that blocks $[A^i_{1,1}]$ and $[A^i_{2,2}]$ are zero; and blocks $[B^i_{1,2}]$ and $[B^i_{2,1}]$ are also zero. Thus, writing only the top G equations of (II.28), we obtain:

$$[J(x_i)] = -[A^{i-1}_{1,2} + A^i_{1,2}]^{-1}\,[B^i_{1,1}]\,[\bar{\phi}_i]$$

$$+ [A^{i-1}_{1,2} + A^i_{1,2}]\,[B^{i-1}_{1,1}]\,[\bar{\phi}_{i-1}] \qquad \text{(II.30)}$$

Using Eq. (II.30) and its counterpart at x_{i+1}, Eq. (II.2) can be transformed into a three-point difference relationship for the average fluxes, as follows:

$$-[A^{i-1}_{1,2} + A^i_{1,2}]^{-1}\,[B^{i-1}_{1,1}]\,[\bar{\phi}_{i-1}]$$

$$+ \left\{[A^{i-1}_{1,2} + A^i_{1,2}]^{-1} + [A^i_{1,2} + A^{i+1}_{1,2}]^{-1}\right\}[B^i_{1,1}]\,[\bar{\phi}_i]$$

$$-[A^i_{1,2} + A^{i+1}_{1,2}]\,[B^{i+1}_{1,1}]\,[\bar{\phi}_{i+1}]$$

$$+ h_i\,[\Sigma_{t_i}]\,[\bar{\phi}_i] = \frac{1}{\lambda}\,h_i\,[\nu\Sigma_{f_i}]^T\,[\bar{\phi}_i] \qquad \text{(II.31)}$$

Equation (II.31) is a matrix equation which can be solved by conventional numerical methods. The values of $[A^{i}_{1,2}]$ and $[B^{i}_{1,1}]$ are derived in Appendix A. The solution of this equation will yield the exact values of the average fluxes in each homogeneous region.

Although Eq. (II.31) has the conventional three-point form, there are two items which make the equation different from the convetional finite difference equations. First, the calculation of the matrices $[A^{i}_{1,2}]$ and $[B^{i}_{1,1}]$ is performed by solving the diffusion equation analytically over each homogeneous region. To solve this equation, the eigenvalue λ of the global problem is required. Therefore, Eq. (II.31) is non-linear, in that improved values of λ are used to re-calculate the coefficient matrices at various times in the static iterative process. Secondly, the coefficient matrices resulting from the substitution of Eq. (II.30) into Eq. (II.2) generally have the same structure as the matrix $[\sum_t(x)] - \frac{1}{\lambda}[\chi][\nu\sum_f(x)]^T$. Therefore, the leakage terms introduce additional group-to-group coupling terms other than those already present due to fissioning and scattering. This is unlike finite difference methods, in which the leakage terms only couple fluxes of one group together.

Comparing Eq. (II.19) to Eq. (II.30), we observe that

$$
\begin{aligned}
[A^{i-1}_{1,2}] &= -[W^{1,1}_{i-1}]^{-1}[W^{1,2}_{i-1}] \\
[A^{i}_{1,2}] &= [U^{1,1}_{i}]^{-1}[U^{1,2}_{i}] \\
[B^{i}_{1,1}] &= -h_i[U^{1,1}_{i}]^{-1}
\end{aligned}
\tag{II.32}
$$

therefore, if regions R_{i-1} and R_i have identical compositions, then

$$-[W^{1,1}_{i-1}]^{-1}[W^{1,2}_{i-1}] = [U^{1,1}_{i}]^{-1}[U^{1,2}_{i}]$$

This demonstrates that the matrices $[U_i]$ and $[W_{i-1}]$ are simply the negative of one another.

E. Extension to Time Dependent Problems

The time-dependent, one-dimensional diffusion equations are

$$[V]^{-1}\frac{\partial}{\partial t}[\phi(x,t)] = \frac{\partial}{\partial x}[D(x,t)]\frac{\partial}{\partial x}[\phi(x,t)] - [\sum_t(x,t)][\phi(x,t)]$$

$$+ [\chi_p] \ (1-\beta) \ [\nu\textstyle\sum_f(x,t)]^T[\phi(x,t)] + \displaystyle\sum_{k=1}^{K} [\chi_{dk}] \ \lambda_k \ C_k(x,t) \qquad \text{(II.33a)}$$

$$\frac{\partial}{\partial t} C_k(x,t) = - \lambda_k \ C_k(x,t) + \beta_k \ [\nu\textstyle\sum_f(x,t)]^T \ [\phi(x,t)] \ (1\underline{<}k\underline{<}K) \qquad \text{(II.33b)}$$

where

$[V]$	is a diagonal G×G matrix containing the neutron speeds
$[\chi_p]$	is a column vector of length G containing the prompt fission spectrum
$[\chi_{dk}]$	is a column vector of length G containing the spectrum from delayed group k
$[\nu\sum_f(x,t)]$	is a column vector of length G containing the critical value of nu times the fission cross section

Integrating Eqs. (II.33) over R_i, we obtain:

$$h_i[V]^{-1} \frac{\partial}{\partial t} [\overline{\phi}_i(t)] = - [J_{i+1}(t)] + [J_i(t)] - h_i \ [\textstyle\sum_{T_i}(t)] \ [\overline{\phi}_i(t)]$$

$$+ h_i \ (1-\beta) \ [\chi_p] \ [\nu\textstyle\sum_{f_i}(t)]^T \ [\overline{\phi}_i(t)] + \displaystyle\sum_{k=1}^{K} [\chi_{dk}] \ \lambda_k \ \overline{C}_{k,i}(t) \qquad \text{(II.34a)}$$

$$\frac{\partial}{\partial t} \overline{C}_{k,i}(t) = - \lambda_k \ \overline{C}_{k,i}(t) + h_i \ \beta_k \ [\nu\textstyle\sum_{f_i}(t)]^T \ [\overline{\phi}_i(t)] \ (1\underline{<}k\underline{<}K) \qquad \text{(II.34b)}$$

where

$$[\overline{\phi}_i(t)] = \frac{1}{h_i} \int_{x_i}^{x_{i+1}} [\phi(x,t)] \ dx$$

$$[J_i(t)] = - [D(x,t)] \frac{\partial}{\partial x} [\phi(x,t)] \Bigg|_{x=x_i}$$

$$[\textstyle\sum_{T_i}(t)] = [\textstyle\sum_T(x,t)] \Bigg|_{x \ \varepsilon \ R_i}$$

$$\bar{C}_{k,i}(t) = \int_{x_i}^{x_{i+1}} C_k(x,t)\, dx$$

$$h_i = x_{i+1} - x_i$$

To obtain a relationship between the net currents and the average fluxes, Eqs. (II.33) must be solved analytically over each homogeneous region. The time derivative and delayed precursor terms complicate this solution, since in general they are not known as a function of x. For assembly-sized mesh spacings, it has been found possible to use the following approximations over the course of a time step. For each region $R_i \equiv (x_i, x_{i+1})$ we assume:

$$\frac{\partial}{\partial t} [\phi(x,t)] = [\omega_{p,i}] [\phi(x,t)] \qquad \text{(II.35a)}$$

$$\frac{\partial}{\partial t} C_k(x,t) = \omega_{dki} C_k(x,t) \qquad \text{(II.35b)}$$

where $[\omega_{p,i}]$ is a diagonal G×G matrix. Inserting Eqs. (II.35) into (II.33) and rearranging, we obtain

$$- \frac{\partial}{\partial x} [D(x,t)] \frac{\partial}{\partial x} [\phi(x,t)]$$

$$+ \left\{ [\textstyle\sum_T(x,t)] + [\omega_{p,i}] \right\} [\phi(x,t)]$$

$$- \left\{ [\chi_p] \; (1-\beta) + \sum_{k=1}^{K} [\chi_{dk}] \left(\frac{\lambda_k \beta_k}{\omega_{dki} + \lambda_k} \right) \right\}$$

$$\cdot \; [\nu \textstyle\sum_f(x,t)]^T [\phi(x,t)] = 0 \qquad \text{(II.36)}$$

If $[\omega_{p,i}]$ and ω_{dki} are known for each region R_i, Eq. (II.36) can be solved analytically at a fixed time t as shown previously. From this analytic solution, an expression of the form of Eq. (II.30) can be obtained. The resulting equation to be solved is then

$$h_i\,[V]^{-1}\frac{\partial}{\partial t}\,[\bar{\phi}_i(t)] \;=\; [A^{i-1}_{1,2} + A^{i}_{1,2}]^{-1}\,[B^{i-1}_{1,1}]\,[\bar{\phi}_{i-1}(t)]$$

$$-\left\{[A^{i-1}_{1,2} + A^{i}_{1,2}]^{-1} + [A^{i}_{1,2} + A^{i+1}_{1,2}]^{-1}\right\}[B^{i}_{1,1}][\bar{\phi}_i(t)]$$

$$+\,[A^{i}_{1,2} + A^{i+1}_{1,2}]^{-1}\,[B^{i+1}_{1,1}]\,[\bar{\phi}_{i+1}(t)] - h_i\,[\textstyle\sum_{T_i}(t)]\,[\bar{\phi}_i(t)]$$

$$+\,h_i(1-\beta)\,[\chi_p]\,[\nu\textstyle\sum_{f_i}(t)]^T\,[\bar{\phi}_i(t)] + \sum_{k=1}^{K}\,[\chi_{dk}]\,\lambda_k\,\bar{C}_{k,i}(t) \qquad \text{(II.37)}$$

Equations (II.37) and (II.34b) can be solved using any conventional numerical method. It should be emphasized that the approximations (II.35) were used only to determine the coupling coefficients; as such they are not expected to introduce a very significant error into the overall solution. The omegas are calculated from

$$\omega_{pgi} = \frac{1}{\Delta T}\,\ell n\left(\bar{\phi}^{n+1}_{gi}\Big/\bar{\phi}^{n}_{gi}\right)$$

$$\omega_{dki} = \frac{1}{\Delta T}\,\ell n\left(\bar{C}^{n+1}_{k,i}\Big/\bar{C}^{n+1}_{k,i}\right)$$

where ΔT is the time step size, g is the energy group index, and n is the time step index.

F. Summary

In this Chapter, a method for solving the one-dimensional, steady-state or transient diffusion equations has been developed. Due to the algebraic complexity of the method (see Appendix A), the scheme in its present form is restricted to one- or two-group problems.

Results of static and transient test problems[7] show that the method is very accurate. For static test problems, the exact result is obtained for both the eigenvalue and eigenvector. For transient test problems, very accurate results have been obtained for spatial mesh regions as large as 20 cm for LWR's. The approximations in Eqs. (II.35) seem to be adequate for reasonable mesh sizes encountered in LWR analysis.

The method used to derive the exact coupling relationships is based on an analytic solution to the diffusion equation. These relationships have been shown to be equivalent to a response matrix derivation of the same problem. In fact, it has been shown how response matrices can be used to calculate coupling coefficients for the nodal solution scheme. This would entail calculating integrals of the reflection and transmission functions. Further work is necessary to develop an efficient computational scheme based on this concept.

III. DEVELOPMENT IN TWO DIMENSIONS

A. Introduction

In Chapter II, a method was developed which produced exact difference equations in one dimension. In two dimensions, it is not clear that exact difference equations exist, or what their matrix structure would be if they did exist. The extension to two dimensions may be performed in two different ways. The first technique is to assume the neutron flux has a multidimensional representation. Some examples of this technique are the finite element method,[6] and the method of Aoki and Tsuiki.[11] The other approach is to assume a one-dimensional representation of the neutron flux. Some examples of this are the Nodal Expansion Method,[3] and a nodal method based on response matrix considerations.[5,9] In the current method, the second approach will be taken. Therefore, the one-dimensional solution to the diffusion equation will be retained, and an estimation of the "transverse leakage" integral required. This derivation is given below.

B. Two Dimensional Derivation

Let us begin in two-dimensional x-y geometry, with a region R defined as

$$R = [0,X] \times [0,Y]$$

and with this region divided into a partition

$$\pi: \quad 0 = x_1, < \ldots < x_I = X$$

$$0 = y_1, < \ldots < y_J = Y$$

We assume that any rectangle defined by the above partition is homogeneous. The two-dimensional diffusion equation is:

$$- \frac{\partial}{\partial x} [D(x,y)] \frac{\partial}{\partial x} [\phi(x,y)] - \frac{\partial}{\partial y} [D(x,y)] \frac{\partial}{\partial y} [\phi(x,y)]$$

$$+ [\Sigma_T(x,y)] [\phi(x,y)] = \frac{1}{\lambda} [\chi] [\nu\Sigma_f(x,y)]^T [\phi(x,y)] \qquad \text{(III.1)}$$

where the terms are defined analagously to those in Eq. (II.1).

When this equation is integrated over (x_i, x_{i+1}) and (y_j, y_{j+1}), we obtain:

$$h_j \left([J_{x_{i+1,j}}] - [J_{x_{i,j}}] \right) + h_i \left([J_{y_{i,j+1}}] - [J_{y_{i,j}}] \right)$$

$$+ h_i h_j \; [\Sigma_{T_{i,j}}] \; [\overline{\phi}_{i,j}] \; = \; \frac{1}{\lambda} h_i h_j \; [\chi] \; [\nu \Sigma_{f_{i,j}}] \; [\overline{\phi}_{i,j}] \qquad \text{(III.2)}$$

where

$$h_i = x_{i+1} - x_i$$

$$h_j = y_{j+1} - y_j$$

$$[\overline{\phi}_{i,j}] = \frac{1}{h_i h_j} \int_{y_j}^{y_{j+1}} \int_{x_i}^{x_{i+1}} [\phi(x,y)] \, dxdy$$

$$[\Sigma_{t_{i,j}}] = [\Sigma_T(x,y)] \Bigg|_{\substack{x \,\varepsilon\, (x_i,\, x_{i+1}) \\ y \,\varepsilon\, (y_j,\, y_{j+1})}}$$

$$[J_{x_{i,j}}] = -\frac{1}{h_j} [D_{i,j}] \frac{\partial}{\partial x} \int_{y_j}^{y_{j+1}} [\phi(x_i,y)] \, dy$$

$$[J_{y_{i,j}}] = -\frac{1}{h_i} [D_{i,j}] \frac{\partial}{\partial y} \int_{x_i}^{x_{i+1}} [\phi(x,y_j)] \, dx$$

The remaining step is to obtain a relationship between the net currents and the average fluxes. This will be accomplished by using the analytical procedure derived in Chapter II.

To illustrate this procedure, let us find a relationship between the x directed net currents and the adjacent average fluxes. To obtain the differential equation which must be solved analytically, we integrate Eq. (II.1) over (y_j, y_{j+1}) and divide by h_j. For $X \in (x_i, x_{i+1})$ we obtain:

$$-[D_{i,j}] \frac{\partial^2}{\partial x^2} [\phi_j(x)] - [D_{i,j}] \int_{y_j}^{y_{j+1}} \frac{1}{h_j} \frac{\partial^2}{\partial y^2} [\phi(x,y)]\, dy$$

$$+ [\Sigma_{T_{i,j}}] [\phi_j(x)] = \frac{1}{\lambda} [\chi] [\nu\Sigma_{f_{i,j}}]^T [\phi_j(x)] \qquad \text{(III.3)}$$

where

$$[\phi_j(x)] = \frac{1}{h_j} \int_{y_j}^{y_{j+1}} [\phi(x,y)]\, dy$$

Equation (III.3) has the same form as the one-dimensional diffusion equation, with the exception of the extra integral representing leakage in the y direction. To solve Eq. (III.3) analytically, this integral must be approximated in some manner. Two possible approximations are:

i) Assume the leakage in the y direction is proportional to the flux in the x direction.

ii) Assume the leakage in the y direction has a low-order polynomial representation.

Assumption i) is the conventional separability assumption. Results using this asumption have been reported in References 7 and 8. For many LWR problems, the separability assumption leads to significant errors. It has been demonstrated in the above references that assumption ii) is preferable.

The most complete study of the various alternatives within assumption ii) has been made by Wagner.[3] In this study, the following functional forms of the leakage integral were studied:

a) The leakage integral is a constant (flat across the node)

b) The leakage integral is a linear function across the node

c) The leakage integral is a quadratic function across the node.

Assumption a) has been studied in detail in Reference 3 and by this author. For many practical problems it yields acceptably accurate results. However, for some extreme test problems, the results are not acceptable. Therefore, a higher order approximation is desired. In References 3 and 5, the quadratic approximation is shown to provide excellent results for all test problems attempted. However, Reference 3 shows that approximation b) also provides acceptably accurate results for the same extreme test problems. Therefore, it may not be necessary to use as complex a representation as assumption c).

In References 3 and 5, the information required to construct a quadratic approximation to the transverse leakage integral is obtained by considering the leakage values over three adjacent nodes. Therefore, although the leakage is approximated as a quadratic function within each node, the same information is used to construct more than one of these quadratic functions. Therefore, it cannot be said that the quadratic approximation to the transverse leakage integral is "complete", since not enough independent pieces of data are available. However, the addition of a modulation on the basic flat shape (even though approximate) appears to significantly improve the accuracy of the results.

In view of the above arguments, two approximations to the transverse leakage integral are developed here. The first is the constant (or flat) leakage approximation. The second is the "two-step" approximation; where the integral is assumed to be flat over each half of the node, however the level of the constant function is different on the left from that on the right. This approximation was chosen instead of assumption b) above since the analytic solution of the diffusion equation is made less complex.

Let us write Eq. (III.3) in a form analagous to Eq. (II.22):

$$\frac{d}{dx}\,[\Phi(x)] + [N]\,[\Phi(x)] = [L(x)] \qquad \text{(III.4)}$$

where we will specify the functional form of [L(x)] later, and

$$[\Phi(x)] = \mathrm{col}\left\{[\phi_j(x)],\ [J_j(x)]\right\}$$

$$[J_j(x)] = -\,[D]\,\frac{d}{dx}\,[\phi_j(x)]$$

$$[L(x)] = \mathrm{col}\left\{[0],\ -\frac{1}{h_j}\,[L_y(x)]\right\}$$

$$[L_y(x)] = -\,[D_{i,j}]\int_{y_j}^{y_{j+1}} \frac{\partial^2}{\partial y^2}\,[\phi(x,y)]\,dy$$

The general solution of Eq. (III.4) at any point x is

$$[\Phi(x)] = e^{-[N](x-x_i)}[\Phi(x_i)]$$

$$+ e^{-[N]x}\int_{x_i}^{x} e^{[N]x'}[L(x')]\, dx' \tag{III.5}$$

Over the interval $R_i \varepsilon (x_i, x_{i+1})$, let us approximate $[L(x)]$ as follows:

$$[L(x)] = \begin{cases} [L_{1,i}] & x_i \leq x \leq x_{i+1/2} \\ \\ [L_{2,i}] & x_{i+1/2} \leq x \leq x_{i+1} \end{cases}$$

This approximation is the "two-step" approximation. We will defer at present a discussion how the values $[L_{1,i}]$ and $[L_{2,i}]$ are obtained. The flat leakage approximation will simply be a special case of the two-step approximation in which $[L(x)] = [L_{1,i}] = [L_{2,i}]$.

Equation (III.5) is next integrated from x_i to x_{i+1} and divided by h_i to obtain:

$$[\bar{\Phi}_i] = \frac{1}{h_i}\int_{x_i}^{x_{i+1}} e^{-[N](x-x_i)}[\Phi(x_i)]\, dx$$

$$+ \frac{1}{h_i}\int_{x_i}^{x_{i+1}} e^{-[N_i]x}\int_{x_i}^{x} e^{[N_i]x'}[L(x')]\, dx'dx$$

where

$$[\bar{\Phi}_i] = \frac{1}{h_i}\int_{x_i}^{x_{i+1}} [\Phi(x)]\, dx$$

$$h_i = x_{i+1} - x_i$$

Next, we insert the above approximation for [L(x)], and carry out the required integrals to obtain:

$$\left\{[I] - e^{-[N_i]h_i}\right\} [\Phi(x_i)] = [N_i]h_i [\bar{\Phi}_i]$$

$$-\left\{\frac{h_i}{2}[I] - [N_i]^{-1}\left([I] - e^{-[N_i]\frac{h_i}{2}}\right)\right\} [L_{1,i}]$$

$$- [N_i]^{-1}\left\{[I] - 2e^{-[N_i]\frac{h_i}{2}} + e^{-[N_i]h_i}\right\} [L_{1,i}]$$

$$-\left\{\frac{h_i}{2}[I] - [N_i]^{-1}\left([I] - e^{-[N_i]\frac{h_i}{2}}\right)\right\} [L_{2,i}] \qquad \text{(III.6)}$$

Next, integrate Eq. (III.5) from x_{i-1} to x_i, and divide by h_{i-1}; where we define [L(x)] as

$$[L(x)] = \begin{cases} [L_{1,i-1}] & x_{i-1} \leq x \leq x_{i-1/2} \\ [L_{2,i-1}] & x_{i-1/2} \leq x \leq x_i \end{cases}$$

After the required integrals are carried out, the following result is obtained:

$$\left\{[I] - e^{[N_{i-1}]h_{i-1}}\right\} [\Phi(x_i)] = - [N_{i-1}]\, h_{i-1} [\bar{\Phi}_{i-1}]$$

$$+\left\{\frac{h_{i-1}}{2}[I] + [N_{i-1}]^{-1}\left([I] - e^{[N_{i-1}]\frac{h_{i-1}}{2}}\right)\right\}[L_{2,i-1}]$$

$$- [N_{i-1}]^{-1}\left\{[I] - 2e^{[N_{i-1}]\frac{h_{i-1}}{2}} + e^{[N_{i-1}]\, h_{i-1}}\right\}[L_{2,i-1}]$$

$$+\left\{\frac{h_{i-1}}{2}\,[I] + [N_{i-1}]^{-1}\left([I] - e^{[N_{i-1}]\frac{h_{i-1}}{2}}\right)\right\}[L_{1,i-1}] \tag{III.7}$$

We now make the following substitutions into Eqs. (III.6) and (III.7):

$$1 - e^{-x} = 1 - \cosh x + \sinh x$$

$$1 - e^{x} = 1 - \cosh x - \sinh x$$

Making these substitutions, we obtain from Eq. (III.6):

$$(\sinh^{-1}[N_i]\,h_i)\left\{[I] - \cosh\,[N_i]\,h_i\right\}[\Phi(x_i] + [\Phi(x_i)]$$

$$= (\sinh^{-1}[N_i]h_i)\,[N_i]\,h_i\,[\bar{\Phi}_i]$$

$$- (\sinh^{-1}[N_i]h_i)\left\{\frac{h_i}{2}\,[I] - [N_i]^{-1}\left([I] - e^{-[N_i]\frac{h_i}{2}}\right)\right\}[L_{1,i}]$$

$$- [N_i]^{-1}\,(\sinh^{-1}[N_i]h_i)\left\{[I] - 2e^{-[N_i]\frac{h_i}{2}} + e^{-[N_i]h_i}\right\}[L_{1,i}]$$

$$- (\sinh^{-1}[N_i]h_i)\left\{\frac{h_i}{2}\,[I] - [N_i]^{-1}\left([I] - e^{-[N_i]\frac{h_i}{2}}\right)\right\}[L_{2,i}] \tag{III.8}$$

and from Eq. (III.7):

$$(\sinh^{-1}[N_{i-1}]h_{i-1})\left\{[I] - \cosh[N_{i-1}]h_{i-1}\right\}[\Phi(x_i)] - [\Phi(x_i)]$$

$$= - (\sinh^{-1}[N_{i-1}]h_{i-1})\,[N_{i-1}]h_i\,[\bar{\Phi}_{i-1}]$$

$$+ (\sinh^{-1}[N_{i-1}]h_{i-1})\left\{\frac{h_{i-1}}{2}\,[I] - [N_{i-1}]^{-1}\left([I] - e^{[N_{i-1}]\frac{h_{i-1}}{2}}\right)\right\}\cdot\,[L_{2,i-1}]$$

$$- [N_{i-1}]^{-1}(\sinh^{-1}[N_{i-1}]h_{i-1}) \left\{[I] - 2e^{[N_{i-1}]\frac{h_{i-1}}{2}} + e^{[N_{i-1}]h_{i-1}}\right\} [L_{2,i-1}]$$

$$+ (\sinh^{-1}[N_{i-1}]h_{i-1}) \left\{\frac{h_{i-1}}{2} [I] + [N_{i-1}]^{-1} \cdot \left([I] - e^{[N_{i-1}]\frac{h_{i-1}}{2}}\right)\right\} \cdot [L_{1,i-1}] \qquad \text{(III.9)}$$

Equation (III.8) and (III.9) are then added together, using the additional relationship

$$(\sinh^{-1}x)\ (1-\cosh x) \ = \ - \tanh \frac{x}{2}$$

to obtain:

$$- \left(\tanh[N_i]\frac{h_i}{2} + \tanh[N_{i-1}]\frac{h_{i-1}}{2}\right) [\Phi(x_i)]$$

$$= (\sinh^{-1}[N_i]h_i)\ [N_i]\ h_i\ [\bar{\Phi}_i] - (\sinh^{-1}[N_{i-1}]h_{i-1})[N_{i-1}]\ h_{i-1}[\bar{\Phi}_{i-1}]$$

$$- (\sinh^{-1}[N_i]h_i) \left\{\frac{h_i}{2} [I] - [N_i]^{-1} \left([I] - e^{-[N_i]\frac{h_i}{2}}\right)\right\}[L_{1,i}]$$

$$- [N_i]^{-1}(\sinh^{-1}[N_i]h_i) \left\{[I] - 2e^{-[N_i]\frac{h_i}{2}} + e^{-[N_i]h_i}\right\} [L_{1,i}]$$

$$- (\sinh^{-1}[N_i]h_i) \left\{\frac{h_i}{2} [I] - [N_i]^{-1} \left([I] - e^{-[N_i]\frac{h_i}{2}}\right)\right\}[L_{2,i}]$$

$$+ (\sinh^{-1}[N_{i-1}]h_{i-1}) \left\{\frac{h_{i-1}}{2} [I] + [N_{i-1}]^{-1} \left([I] - e^{[N_{i-1}]\frac{h_{i-1}}{2}}\right)\right\}[L_{2,i-1}]$$

$$- [N_{i-1}]^{-1}(\sinh^{-1}[N_{i-1}]h_{i-1}) \left\{[I] - 2e^{[N_{i-1}]\frac{h_{i-1}}{2}} + e^{[N_{i-1}]h_{i-1}}\right\}[L_{2,i-1}]$$

$$+ (\sinh^{-1}[N_{i-1}]h_{i-1})\left\{\frac{h_{i-1}}{2}[I] + [N_{i-1}]^{-1}\right.$$

$$\left.\cdot\left([I] - e^{[N_{i-1}]\frac{h_{i-1}}{2}}\right)\right\}[L_{1,i-1}] \tag{III.10}$$

Next, we use the relationships

$$[L_{s,i}] = \frac{1}{2}\left\{[L_{i,i}] + [L_{2,i}]\right\} \tag{III.11}$$

$$[L_{d,i}] = \frac{1}{2}\left\{[L_{1,i}] - [L_{2,i}]\right\}$$

or

$$[L_{1,i}] = [L_{s,i}] + [L_{d,i}]$$

$$[L_{2,i}] = [L_{s,i}] - [L_{d,i}]$$

Equation (III.10) then becomes:

$$- \left(\tanh[N_i]\frac{h_i}{2} + \tanh[N_{i-1}]\frac{h_{i-1}}{2}\right)[\Phi(x_i)]$$

$$= (\sinh^{-1}[N_i]h_i)[N_i]h_i[\bar{\Phi}_i] - (\sinh^{-1}[N_{i-1}]h_{i-1})[N_{i-1}]h_{i-1}[\bar{\Phi}_{i-1}]$$

$$- (\sinh^{-1}[N_i]h_i)\left\{h_i[I] - [N_i]^{-1}\left([I] - e^{-[N_i]h_i}\right)\right\}[L_{s,i}]$$

$$- [N_i]^{-1}(\sinh^{-1}[N_i]h_i)\left\{[I] - 2e^{-[N_i]\frac{h_i}{2}} + e^{-[N_i]h_i}\right\}[L_{d,i}]$$

$$+ (\sinh^{-1}[N_{i-1}]h_{i-1}) \left\{h_{i-1}[I] + [N_{i-1}]^{-1}\left([I] - e^{[N_{i-1}]h_{i-1}}\right)\right\}[L_{s,i-1}]$$

$$+ [N_{i-1}]^{-1}(\sinh^{-1}[N_{i-1}]h_{i-1}) \left\{[I] - 2e^{[N_{i-1}]\frac{h_{i-1}}{2}}\right.$$

$$\left. + e^{[N_{i-1}]h_{i-1}}\right\} [L_{d,i-1}] \qquad \text{(III.12)}$$

At this point, some further algebraic manipulation of Eq. (III.12) is required. The following definitions can be made:

$$[A^i] = \tanh [N_i] \frac{h_i}{2} \qquad \text{(III.13a)}$$

$$[B^i] = (\sinh^{-1}[N_i]h_i)\ [N_i]h_i \qquad \text{(III.13b)}$$

Next, the term multiplying $[L_{s,i}]$ will be rearranged. Let us write the term

$$- (\sinh^{-1}[N_i]h_i) \left\{h_i[I] - [N_i]^{-1}\left([I] - e^{-[N_i]h_i}\right)\right\}$$

using the relationship

$$1 - e^{-x} = 1 - \cosh x + \sinh x$$

This term becomes:

$$- (\sinh^{-1}[N_i]h_i) \left\{h_i[I] - [N_i]^{-1}\left([I] - \cosh[N_i]h_i\right)\right\} + [N_i]^{-1}$$

Using the nomenclature of Appendix A, this term can be shown to be:

$$- \begin{bmatrix} E_{11} & 0 \\ 0 & E_{22} \end{bmatrix} \begin{bmatrix} 0 & H_{21}^{-1}(h) \\ H_{12}^{-1}(h) & 0 \end{bmatrix} \begin{bmatrix} E_{11}^{-1} & 0 \\ 0 & E_{22}^{-1} \end{bmatrix} \left\{ \begin{bmatrix} h_i & 0 \\ 0 & h_i \end{bmatrix} \right.$$

$$\left. - \begin{bmatrix} 0 & N_{21}^{-1} \\ N_{12}^{-1} & 0 \end{bmatrix} \left(\begin{bmatrix} I & 0 \\ 0 & I \end{bmatrix} - \begin{bmatrix} K_{11}(h) & 0 \\ 0 & K_{22}(h) \end{bmatrix} \right) \right\} + \begin{bmatrix} 0 & N_{21}^{-1} \\ N_{12}^{-1} & 0 \end{bmatrix}$$

where $[K(h)] \; = \; \cosh\, [N_i]\, h_i$.

We note that this expression (which represents $2G \times 2G$ matrices) will multiply a column vector whose first G entries are all zero. Therefore, the entries (1,1) and (2,1) in the resulting expression above are not needed. In addition, only the top G equations will be used in the final expression. Therefore, only element (1,2) is required. We may then reduce the original term above to

$$[D^i] \; = \; - (\sinh^{-1}[N_i]h_i)\, h_i + [N_i]^{-1} \qquad \text{(III.13c)}$$

where the (1,2) element of Eq. (III.13c) is the same as the (1,2) element of the original expression. An analogous simplification of the term multiplying $[L_{s,i-1}]$ reduces to the same form as Eq. (III.13c) above. Therefore, Eq. (III.13c) is correct in general for all i.

The terms which multiply $[L_{d,i-1}]$ and $[L_{d,i}]$ do not at first appear to represent the same term; however after simplification their (1,2) elements can be shown to be the same. Important in this simplification are the trigonometric relationships

$$(\sinh^{-1}x)\; (1-\cosh \tfrac{x}{2} + \sinh \tfrac{x}{2})^2 \; = \; \tfrac{1}{2} \tanh \tfrac{x}{2}\; (1-\tanh \tfrac{x}{4})^2$$

$$(\sinh^{-1}x)\; (1-\cosh \tfrac{x}{2} - \sinh \tfrac{x}{2})^2 \; = \; \tfrac{1}{2} \tanh \tfrac{x}{2}\; (1+\tanh \tfrac{x}{4})^2$$

The final result is

$$[F^i] \; = \; [N_i]^{-1} \left(\frac{1}{2}\right) \left(\tanh[N_i]\frac{h_i}{2}\right) \left([I] - \tanh[N_i]\, \frac{h_i}{4}\right)^2 \qquad \text{(III.13d)}$$

The expressions Eq. (III.13a,b,c,d) are evaluated in Appendix A for both one- and two-neutron energy groups.

Taking only the top G equations of Eq. (III.12), and using the definitions Eqs. (III.13), we obtain:

$$- \left([A^{i-1}_{1,2}] + [A^{i}_{1,2}] \right) \; [J(x_i)] \; = \; [B^{i}_{1,1}] \; [\bar{\phi}_i] - [B^{i-1}_{1,1}] \; [\bar{\phi}_{i-1}]$$

$$- [D^{i}_{1,2}] \; [Lk_{s,i}] + [D^{i-1}_{1,2}] \; [Lk_{s,i-1}] \qquad \text{(III.14)}$$

$$- [F^{i}_{1,2}] \; [Lk_{d,i}] - [F^{i-1}_{1,2}] \; [Lk_{d,i-1}]$$

where the [Lk] terms represent the lower G entries in the vector [L].

Equation (III.14) is a matrix equation relating the x-directed current at x_i to the adjacent average fluxes. In addition, it can be seen that the current at x_i depends on the y-directed leakage in the adjacent regions. Therefore, if Eq. (III.14) is substituted into Eq. (III.2) for both the x- and y-directed currents, the current terms would not be completely eliminated from the equation; as was the case in one dimension. Thus, in two or more dimensions, the equations for both the average neutron fluxes and the currents must be solved simultaneously. In the next Section, the matrix structure of the resulting equations will be shown.

C. Matrix Structure of Equations

Let us rewrite Eq. (III.2) as follows:

$$h_j [L_{x_{i,j}}] + h_i \; [L_{y_{i,j}}] + h_i h_j \; [\textstyle\sum_{T_{i,j}}] \; [\bar{\phi}_{i,j}]$$

$$= \frac{1}{\lambda} \; [\chi] \; [\nu \textstyle\sum_{f_{i,j}}]^T \; [\bar{\phi}_{i,j}] \qquad \text{(III.15)}$$

where

$$[L_{x_{i,j}}] \; = \; [J_{x_{i+1,j}}] - [J_{x_{i,j}}]$$

$$[L_{y_{i,j}}] \; = \; [J_{y_{i,j+1}}] - [J_{y_{i,j}}]$$

From Eq. (III.14), we obtain

$$[L_{x_{i,j}}] = -[C^{i,i-1}_{x,j}]\,[\bar{\phi}_{i-1,j}]$$

$$+[C^{i,i}_{x,j}]\,[\bar{\phi}_{i,j}] - [C^{i,i+1}_{x,j}]\,[\bar{\phi}_{i+1,j}]$$

$$+\frac{1}{h_j}\,[E^{i,i-1}_{x,j}]\,[Lk_{s,i-1}] - \frac{1}{h_j}\,[E^{i,i}_{x,j}]\,[Lk_{x_{s,i}}]$$

$$+\frac{1}{h_j}\,[E^{i,i+1}_{x,j}]\,[Lk_{x_{s,i+1}}]$$

$$-\frac{1}{h_j}\,[G^{i,i-1}_{x,j}]\,[Lk_{x_{d,i-1}}] + \frac{1}{h_j}\,[G^{i,i}_{x,j}]\,[Lk_{x_{d,i}}]$$

$$+\frac{1}{h_j}\,[G^{i,i+1}_{x,j}]\,[Lk_{x_{d,i+1}}] \qquad \text{(III.16)}$$

where

$$[C^{i,i-1}_{x,j}] = \left([A^{i-1}_{1,2}] + [A^{i}_{1,2}]\right)^{-1} [B^{i-1}_{1,1}]$$

$$[C^{i,i}_{x,j}] = \left\{\left([A^{i-1}_{1,2}] + [A^{i}_{1,2}]\right)^{-1} + \left([A^{i}_{1,2}] + [A^{i+1}_{1,2}]\right)^{-1}\right\} [B^{i}_{1,1}]$$

$$[C^{i,i+1}_{x,j}] = \left([A^{i}_{1,2}] + [A^{i+1}_{1,2}]\right)^{-1} [B^{i+1}_{1,1}]$$

$$[E^{i,i-1}_{x,j}] = \left([A^{i-1}_{1,2}] + [A^{i}_{1,2}]\right)^{-1} [D^{i-1}_{1,2}]$$

$$[E^{i,i}_{x,j}] = \left\{\left([A^{i-1}_{1,2}] + [A^{i}_{1,2}]\right)^{-1} + \left([A^{i}_{1,2}] + [A^{i+1}_{1,2}]\right)^{-1}\right\} [D^{i}_{1,2}]$$

$$[E_{x,j}^{i,i+1}] = \left([A_{1,2}^{i}] + [A_{1,2}^{i+1}]\right)^{-1} [D_{1,2}^{i+1}]$$

$$[G_{x,j}^{i,i-1}] = \left([A_{1,2}^{i-1}] + [A_{1,2}^{i}]\right)^{-1} [F_{1,2}^{i-1}]$$

$$[G_{x,j}^{i,i}] = \left\{- \left([A_{1,2}^{i-1}] + [A_{1,2}^{i}]\right)^{-1} + \left([A_{1,2}^{i}] + [A_{1,2}^{i+1}]\right)^{-1}\right\} [F_{1,2}^{i}]$$

$$[G_{x,j}^{i,i+1}] = \left([A_{1,2}^{i}] + [A_{1,2}^{i+1}]\right)^{-1} [F_{1,2}^{i+1}]$$

An analogous expression holds for $[L_{y_{i,j}}]$.

Substitution of Eq. (III.16) and the analogous expression for $[L_{y_{i,j}}]$ into Eq. (III.15) yields:

$$- h_j[C_{x,j}^{i,i-1}]\ [\bar{\phi}_{i-1,j}] - h_i[C_{y,i}^{j,j-1}]\ [\bar{\phi}_{i,j-1}]$$

$$- h_j[C_{x,j}^{i,i+1}]\ [\bar{\phi}_{i+1,j}] - h_i[C_{y,i}^{j,j+1}]\ [\bar{\phi}_{i,j+1}]$$

$$+ \left(h_j[C_{x,j}^{i,i}] + h_i[C_{y,i}^{j,j}] + h_i h_j[\textstyle\sum_{T_{i,j}}]\right) [\bar{\phi}_{i,j}]$$

$$= \frac{1}{\lambda}\ [\chi]\ [\nu \textstyle\sum_{f_{i,j}}]^{T}\ [\bar{\phi}_{i,j}]$$

$$- \left\{[E_{x,j}^{i,i-1}]\ [Lk_{x_{s,i-1}}] - [E_{x,j}^{i,i}]\ [Lk_{x_{s,i}}] + [E_{x,j}^{i,i+1}]\ [Lk_{x_{s,i+1}}]\right.$$

$$- [G_{x,j}^{i,i-1}]\ [Lk_{x_{d,i-1}}] + [G_{x,j}^{i,i}]\ [Lk_{x_{d,i}}] + [G_{x,j}^{i,i+1}]\ [Lk_{x_{d,i+1}}]$$

$$+ [E_{y,i}^{j,j-1}]\ [Lk_{y_{s,j-1}}] - [E_{y,i}^{j,j}]\ [Lk_{y_{s,j}}] + [E_{y,i}^{j,j+1}]\ [Lk_{y_{s,j+1}}]$$

$$- [G_{y,i}^{j,j-1}] [Lk_{y_{d,j-1}}] + [G_{y,i}^{j,j}] [Lk_{y_{d,j}}] + [G_{y,i}^{j,j+1}] [Lk_{y_{d,j+1}}] \Bigg\} \qquad \text{(III.17)}$$

Equation (III.17) is solved in a conventional manner, using a fission source iteration accelerated by the use of Chebyshev polynomials. The "inner" iterations to solve for the average fluxes at each mesh point and outer iteration are performed using the cyclic Chebyshev iterative method. Both neutron energy groups (in two-group problems) are solved simultaneously. References 7 and 8 contain a more detailed discussion of the solution techniques.

The calculation of the terms [Lk] has not yet been discussed. Because of Eq. (III.11), it can be shown that

$$[Lk_{x_{s,i}}] = [L_{y_{i,j}}] \qquad \text{(III.18a)}$$

$$[Lk_{y_{s,j}}] = [L_{x_{i,j}}] \qquad \text{(III.18b)}$$

Thus, the average leakage required in the x-directed analytical solution is the average y-directed leakage; and the average leakage required in the y-directed analytical solution is the average x-directed leakage.

To calculate the

$[Lk_{x_{d,i}}]$ and $[Lk_{y_{d,j}}]$

terms, straight lines are drawn between the adjacent regions. The following expressions are used:

$$[Lk_{x_{d,i}}] = \frac{1}{2} \Bigg\{ [L_{y_{i-1,j}}] - [L_{y_{i+1,j}}] + F_{x_\ell} \left([L_{y_{i,j}}] - [L_{y_{i-1,j}}] \right) - F_{x_r} \left([L_{y_{i,j}}] - [L_{y_{i+1,j}}] \right) \Bigg\} \qquad \text{(III.18c)}$$

$$[Lk_{y_{d,j}}] = \frac{1}{2} \Bigg\{ [L_{x_{i,j-1}}] - [L_{x_{i,j+1}}] + F_{y_\ell} \left([L_{x_{i,j}}] - [L_{x_{i,j-1}}] \right)$$

$$+ F_{y_r}\left([L_{x_{i,j}}] - [L_{x_{i,j+1}}]\right)\Bigg\} \qquad \text{(III.18d)}$$

where

$$F_{x_\ell} = \frac{\frac{1}{2}h_i + h_{i-1}}{h_{i-1} + h_i}$$

$$F_{x_r} = \frac{\frac{1}{2}h_i + h_{i+1}}{h_i + h_{i+1}}$$

$$F_{y_\ell} = \frac{\frac{1}{2}h_j + h_{j-1}}{h_j + h_{j-1}}$$

$$F_{y_r} = \frac{\frac{1}{2}h_j + h_{j+1}}{h_j + h_{j+1}}$$

The overall steady-state solution procedure is then:

a) An accelerated fission source iteration is used to calculate the eigenvalue and eigenfunction.

b) At each "outer" iteration, Eq. (III.17) is solved to calculate the average fluxes.

c) Equation (III.16) and its counterpart for $[L_{y_{i,j}}]$ are solved to calculate the new average leakages.

d) If the two-step method is being used, Eqs. (III.18c and d) are solved to calculate the $[Lk_{x_{d,i}}]$ and $[Lk_{y_{d,j}}]$ terms.

As can be seen above, the calculational sequence at each outer iteration involves both an iterative solution to determine the average fluxes, and the calculation of the leakage terms. The matrix

$$h_j[C_x] + h_i[C_y] + h_ih_j[\Sigma_{T_{i,j}}]$$

which must be inverted at every outer iteration (from Eq. III.17) is generally relatively easy to invert, especially for assembly-sized mesh spacings. It is common that only a few (two or three) cyclic Chebyshev iterations are required to invert this matrix. Therefore, about as much computational effort is expended to calculate the leakages at every outer iteration as is expended to invert the above matrix and calculate the average fluxes.

To accelerate the convergence of the outer iterations further, it is possible to use Weilandt's method of fractional iterations.[12] This method is illustrated below for a simple problem. Let

$$[C]\ [\phi] = \frac{1}{\lambda}\ [M]\ [\phi] \qquad \text{(III.19)}$$

be an eigenvalue problem. Then choose a value λ_s such that $\lambda_s > \lambda$. Then subtract $\frac{1}{\lambda_s}$ [M] [ϕ] from the above equation to obtain

$$\left\{[C] - \frac{1}{\lambda_s}[M]\right\}\ [\phi] = \left(\frac{1}{\lambda} - \frac{1}{\lambda_s}\right)\ [M]\ [\phi]$$

Next, define

$$\frac{1}{\lambda_{new}} = \frac{1}{\lambda} - \frac{1}{\lambda_s},$$

so

$$\left\{[C] - \frac{1}{\lambda_s}[M]\right\}\ [\phi] = \frac{1}{\lambda_{new}}\ [M]\ [\phi] \qquad \text{(III.20)}$$

Instead of solving Eq. (III.19), we choose to solve Eq. (III.20). This choice is motivated by the following observations:

a) The spectral radius of the Jacobi iteration matrix is larger for the matrix

$$\left\{[C] - \frac{1}{\lambda_s}[M]\right\}$$

then it is for the matrix [C].[12] In fact, in the limit of $\lambda_s = \lambda$, the spectral radius of

$$\left\{[C] - \frac{1}{\lambda_s} [M]\right\}$$

is one.

b) The dominance ratio (ratio of second to first eigenvalue) of the outer iteration matrix in Eq. (III.20) is lower than that of Eq. (III.19). Therefore, although the matrix to be inverted at each outer iteration is more difficult in Eq. (III.20); it should require fewer outer interations to converge. Therefore, Weilandt's method was implemented into the steady-state solution in the following manner. At the beginning of the steady-state solution, the user enters an estimate of the eigenvalue λ. This estimate is used in the calculation of the matrices (Appendix A). The search eigenvalue, λ_s, is obtained from

$$\frac{1}{\lambda_s} = \frac{W_f}{\lambda_{est}}$$

where λ_{est} is the input estimate, and W_f is a user input value ($0 \leq W_f < 1.0$). The same value of λ_s was kept for the entire steady-state iteration. The convergence of Eq. (III.20) was accelerated by the use of Chebyshev polynomials. At the conclusion of the steady-state iterative process, the eigenvalue λ was calculated from

$$\frac{1}{\lambda} = \frac{1}{\lambda_{new}} - \frac{1}{\lambda_s}$$

or

$$\lambda = \frac{\lambda_{new}\lambda_s}{\lambda_{new}+\lambda_s} \qquad \text{(III.21)}$$

To investigate what value of W_f to use, a variety of runs were made using the BIBLIS test problem (Section IV.B.4). Table I shows the results of this study. The input eigenvalue estimate was 1.025. Although there are local oscillations, Table I demonstrates that the Weilandt iteration is effective in reducing the number of outer iterations, and the overall execution time.

As a result of this and other test problems, it was decided that the factor 0.9 should be used for W_f as a general rule. In the case where the user does not know to any degree of certainty what the final eigenvalue will be, this factor should insure that $\lambda_s > \lambda$. If the eigenvalue is completely unknown, a value of 0.75 can be used to be completely safe.

TABLE I. Investigation of Weilandt Iteration

Weilandt Factor W_f	λ_s	Number of Outer Iterations	Number of Inner/Outer	Execution Time (sec) (370/195)
0.0	(undef.)	47	2	1.044
0.2	5.125	48	2	1.088
0.4	2.56	41	3	1.042
0.6	1.708	44	3	1.077
0.7	1.464	35	3	0.857
0.8	1.280	33	4	0.881
0.9	1.139	23	5	0.665
0.95	1.079	22	6	0.702

For the test problems to be shown in Chapter IV, a Weilandt factor of $W_f = 0.9$ was used. As with the BIBLIS case shown in Table I, this reduced the execution time for steady-state solution by as much as 40% for those problems.

D. Time Dependent Solution

The same techniques used in Section (II.E) are used in two dimensions. The approximations (II.35) are used to derive an equation which may be solved analytically as was done in the previous section. The time integration method used is the fully implicit method. The same solution techniques are used as described in References 7 and 8, with one major exception detailed below.

At each time step of a transient, it has been previously felt that the coefficient matrices must be re-calculated; since the cross section and [ω] terms change during this transient. In Reference 7, it was shown that this re-calculation of the coefficient matrices required a large percentage of the calculation time of a transient; for some cases up to 55%. If the coefficient matrices need only be re-calculated every two or three time steps, a significant savings in execution time could be realized. It was therefore attempted to re-calculate the coefficient matrices every n time steps during a transient. The necessary changes to [$\Sigma_{T_{i,j}}$] due to external perturbations and thermal feedback are made every time step. The results of these studies show that the coefficient matrices may be re-calculated every three or four time steps without a significant decrease in accuracy. Due to the success of this scheme for even a very severe test problem, (see Section IV.C) it is felt that a re-calculation of the coefficient matrices every 3 time steps is adequate in the general case.

IV. RESULTS

A. Introduction

In this Chapter, results from four steady-state and one transient, two-dimensional benchmark problems are given. These problems are designed to show the accuracy and efficiency of both of the methods developed here.

B. Static Benchmark Problems

Four static, two-dimensional, two-group benchmark problems are discussed in this Section. They range from a relatively simple two-region problem to a checkerboard-loaded PWR.

1. Two-Region Test Problem

This two-region problem first appeared in Reference 6, which discusses finite element methods. The geometric configuration and macroscopic cross sections are presented in that reference.

In Figure 1, the inverse eigenvalues ($1/\lambda$) for both the flat leakage and two-step method are presented. Results are also given for Kang's cubic Hermite polynomials. The results obtained from the two-step method are clearly superior to those from the flat leakage method for this problem. The two-step method and the cubic Hermite method are both able to give very accurate results using a large mesh spacing. For all methods, an order of convergence is shown. The two-step method shows a significantly higher order of convergence than the flat leakage method; although it is doubtful that any specific order of convergence could be proved mathematically to be expected for the nodal schemes.

ΔX	Cubic Hermite Method	NODAL ANALYTIC METHOD	
		Flat Leakage	Two-Step Leakage
L/4	1.1134916	1.1118268	1.1135889
L/6	1.140943	1.1131629	1.1140013
L/8	-	1.1136451	1.1141208
L/16	-	-	1.1142363
Order of Convergence	3.2	2.0	2.5

Fig. 1. Eigenvalues ($1/\lambda$) for Two-Region Test Problem
ANL Neg. No. 116-78-182

2. LRA Benchmark Problem

This benchmark problem is representative of a BWR; and forms the initial conditions for the transient benchmark problem described as Benchmark Source Situation BSS-14 of Reference 10. Figure 2 shows the eigenvalues and errors in the initial power distributions for both the flat leakage and two-step leakage methods. For both schemes, the maximum assembly power errors are below 3%. The two-step method yields very accurate results for this problem; with the maximum assembly power error below 1%. For this problem, the reference solution is taken as a two-step solution using a 3.75 cm mesh. Steady-state runs using various mesh sizes have demonstrated the accuracy of this solution.

(Normalized Reference Powers and Percent Errors)

Execution Time (sec)*		Eigenvalue (λ)
	Reference	0.996360
2.47	Flat	0.996944
2.55	Two-Step	0.996553

							1.328 2.6 0.6	
						2.161 2.8 0.8	1.621 2.3 0.6	0.8465 1.2 0.2
					1.852 1.9 0.5	2.051 2.3 0.7	1.679 1.7 0.4	0.9716 1.8 0.6
				0.8643 0.4 0.2	1.152 -0.1 -0.2	1.339 0.2 -0.1	1.422 1.3 0.4	0.9325 1.6 0.4
			0.5524 0.1 0.1	0.6782 -0.3 -0.1	0.8432 -1.3 -0.4	1.022 -1.1 -0.3	1.221 -0.1 -0.1	0.8530 0.7 0.2
		0.4240 -0.6 -0.1	0.4921 -0.3 -0.1	0.6181 -0.8 -0.2	0.7826 -1.9 -0.5	0.9667 -1.8 -0.5	1.173 -1.0 -0.3	0.8268 -0.3 -0.1
	0.3995 -1.8 -0.4	0.4067 -1.6 -0.5	0.4921 -0.3 -0.1	0.6705 -0.8 -0.1	0.9398 -1.5 -0.5	1.151 -1.6 -0.5	1.281 -0.9 -0.2	0.8672 -1.0 -0.3
0.6122 -1.1 -0.2	0.4402 -2.6 -0.8	0.4130 -3.0 -0.8	0.5118 -2.7 -0.7	0.7902 -1.9 -0.6	1.386 -0.1 0	1.661 0 0.1	1.481 -1.4 -0.3	0.9242 -2.0 -0.5

*Times measured on IBM 370/168
Convergence -10^{-5} on pointwise flux

Fig. 2. Power Distribution for the LRA Benchmark Problem
ANL Neg. No. 116-78-158

3. IAEA Benchmark Problem

This well known benchmark problem is representative of a PWR. The geometric configuration and macroscopic cross sections are given in Reference 7. Figure 3 shows the eigenvalues and errors in the power distributions for both the flat leakage and two-step leakage methods. For the flat leakage method, the maximum assembly power error is less than 3%; for the two-step leakage method, the maximum error is less than 2.0%. The eigenvalue is also significantly improved by using the two-step approximation. The reference solution is taken from an exptrapolated series of finite-difference solutions.[13]

(Normalized Reference Powers and Percent Errors)*

Execution Time (sec)**		Eigenvalue λ
	Reference	1.02959
1.32	Flat	1.03001
1.41	Two-Step	1.02970

Coarse Mesh Size - 20 cm

					0.585 0.2 -0.3		
				0.471 -1.5 -0.6	0.685 2.8 1.6	0.598 1.8 0.7	
			1.192 -0.3 -0.1	0.966 0.6 0.5	0.906 0.8 0.3	0.847 0.6 0.1	
		1.469 -1.4 -0.3	1.345 -0.7 0	1.179 0.8 0.3	1.071 -0.3 -0.2	0.976 -0.1 -0.2	0.692 -0.3 -0.6
	1.435 -0.6 -0.1	1.479 -0.7 -0.1	1.314 -0.4 -0.1	1.070 0.2 0.2	1.036 -0.4 -0.3	0.951 -0.4 -0.4	0.736 0.1 -0.4
0.746 -2.5 -0.5	1.308 -0.2 -0.2	1.454 0.6 0.1	1.210 0.1 0.2	0.610 -2.3 -0.7	0.935 0.2 0.1	0.934 0.4 -0.1	0.755 0.1 -0.7

*Convergence criteria is 10^{-5} on pointwise flux
**Times measured relative to an IBM 370/168

Fig. 3. Power Distribution for the IAEA Benchmark Problem
ANL Neg. No. 116-78-180

4. BIBLIS Benchmark Problem

The BIBLIS benchmark problem is representative of a PWR with a checkerboard fuel loading. The specific configuration solved is the "rods out" configuration. This problem is a very difficult one to solve because of the large mesh sizes (23 cm) and the checkerboard fuel loading pattern. The geometric configuration and macroscopic cross sections unfortunately cannot be published due to company confidentiality restrictions.

Figure 4 contains the eigenvalues and errors in power distribution for both the flat leakage and two-step leakage methods. For this problem, the flat leakage results are not acceptable; with errors in assembly powers as large as 8.9%. The two-step method, however, provides acceptably accurate results; with the maximum error in assembly power being 4.0%.

(Normalized Reference Powers and Percent Errors)*

Execution Time (sec)**		Eigenvalue λ
	Reference	1.02512
1.57	Flat	1.02585
1.66	Two-Step	1.02549

					1.202 8.9 4.0	0.6863 8.8 3.1	
				1.124 2.1 1.1	0.9942 4.5 1.9	0.8765 7.7 3.5	
			1.161 -0.9 -0.2	1.039 -0.4 -0.3	0.9509 1.2 0.8	0.7653 1.9 0.9	0.5459 4.5 2.4
		1.122 -3.2 -1.2	1.104 -2.8 -1.3	1.120 -1.1 -0.3	0.9232 -1.3 -0.7	0.9308 0.5 0.4	0.8240 2.9 1.2
	1.117 -3.9 -1.6	1.133 -3.9 -1.8	1.223 -2.8 -1.1	1.067 -2.9 -1.4	1.032 -1.4 -0.5	1.071 0 -0.2	0.9694 0.8 0.1
1.090 -4.7 -1.9	1.101 -4.8 -2.2	1.242 -3.2 -1.4	1.220 -3.4 -1.6	1.088 -2.8 -1.0	0.9812 -2.1 -1.0	1.094 -0.3 -0.3	1.013 0.6 0

*Convergence criteria is 10^{-5} on pointwise flux
**Times measured relative to an IBM 370/168

Fig. 4. Power Distribution for the BIBLIS Benchmark Problem
ANL Neg. No. 116-78-181

5. Summary of Static Benchmark Problems

An examination of Figures 1 through 4 show the following general trends:

a) The two-step method provides consistently better results than the flat leakage method.

b) The two-step method generally requires no more than a 20% increase in execution time over the flat leakage method.

c) The two-step method provides results of acceptable accuracy for all the test cases shown here.

C. Transient Benchmark Problem

The transient benchmark problem described here is Benchmark Source Situation BSS-14 of Reference 10. The geometric configuration and macroscopic cross sections are given in Reference 10. For this problem, three solutions are provided:

a) Coarse-mesh solution using flat leakage approximation
b) Coarse-mesh solution using two-step leakage approximation
c) Reference solution using two-step leakage approximation.

The transient consists of the ramp removal of a rod over $0 < t < 2.0$ sec. Adiabatic fuel temperature feedback is included; it modifies the fast group absorption cross section. The solution is followed to 3.0 seconds.

The reference solution for this transient has been calculated using the two-step method using a 7.5 cm mesh. Steady-state results show that this solution has an eigenvalue error of 0.005% and a maximum error in assembly power of 0.3%. The reference solution required 2600 time steps to insure that the temporal truncation error was small. The following time domains were used:

1) 200 steps with ΔT = 0.005 sec
2) 600 steps with ΔT = 0.0005 sec
3) 1200 steps with ΔT = 0.00025 sec
4) 400 steps with ΔT = 0.001 sec
5) 200 steps with ΔT = 0.005 sec

The matrices were calculated every time step. Figure B.1 shows the assembly powers and temperatures at various times during the transient. The core average powers and temperatures are also shown.

The coarse mesh solutions were calculated using a 15 cm mesh. The steady-state results for both the two-step and flat leakage methods are given in Figure 2. The coarse mesh solutions required 1000 time steps. The following time domains were used for both coarse mesh solutions:

1) 100 steps with ΔT = 0.01 sec
2) 300 steps with ΔT = 0.001 sec
3) 400 steps with ΔT = 0.0005 sec
4) 100 steps with ΔT = 0.005 sec
5) 100 steps with ΔT = 0.01 sec

For both coarse mesh solutions, the coefficient matrices were re-calculated every four time steps. Figure B.2 shows the assembly powers and temperatures at various times during the transient for the two-step leakage method. Figure B.3 shows the assembly powers and temperatures at various times during the transient for the flat leakage method.

Several runs were made to explore the errors introduced by re-calculating the coefficient matrices every four time steps, rather than every time step.

The error in global parameters, such as total power, is small; generally being 0.6% or less. Errors in individual assembly powers were generally less than 1%.

Table II compares the three solutions for some key parameters during the transient. The two-step leakage method is seen to provide acceptably accurate results for this problem. Table III contrasts the results from a number of investigators against the two-step leakage method and the reference solution. The execution time for the two-step leakage method (210 sec on IBM 370/168) compares well with those of the CUBBOX[4] code (180 sec on IBM 360/91) and the IQSBOX[3] code (255 sec on CYBER 175[10]). The solutions obtained by the two-step method in Figure B.2 compare well with the solutions presented from the CUBBOX and IQSBOX codes presented in Reference 10.

TABLE II. Summary of Results for BWR Kinetics Benchmark Problem

	Coarse Mesh Analytic Solution[a] (Flat Leakage)	Coarse Mesh Analytic Solution[a] (Two-Step)	Reference Solution[b]
1) Time to first peak (sec)	1.403	1.426	1.436
2) Mean Power at first peak (w/cc)	5567	5552	5411
3) Time to second peak (sec)	2.0	2.0	2.0
4) Mean Power at second peak (w/cc)	825	815	784
5) Maximum assembly power error at t=0.0 sec (%)	3.0	0.8	0.3
6) Maximum temperature at t=3.0 sec (°K)	3261	3112	2948
7) Average temperature at t=3.0 sec (°K)	1155	1127	1087
8) Number of time steps	1000	1000	2600
9) Execution time (sec) on 370/168	185	210	4152

[a]Coarse mesh solution use 15 cm mesh.

[b]Reference solution is 2-step method with 7.5 cm mesh.

Figure 5 shows the mean power versus time for the reference solution. The power is observed to rise over ten orders of magnitude, until the temperature feedback provides enough excess reactivity to halt the power increase. The power oscillation is typical of kinetics problems with temperature feedback.

Figure 6 compares the mean powers for the reference solution (circle symbol o) and the two-step leakage solution (square symbol □) over the interval $1.3 \leq t \leq 2.0$ sec. This figure shows that the two-step method provides acceptably accurate results.

The efficiency of the methods developed in this report can be best demonstrated by contrasting them with finite difference methods. For this problem, a mesh-centered finite difference code such as MEKIN[14] requires a (6 × 6) mesh within each 15 cm assembly to achieve a maximum error of 5% in the steady-state power distribution inside each assembly. Therefore, for 1000

TABLE III. Comparison of Results for BWR Test Problem

	Werner[4]	Finnemann[3]	Shober	Sims[5]	Reference
Number of Time Steps	1200	522	1000	1300	2600
CPU Time (sec) (Computer)	180 360/91	255 CYBER 175	210 370/168	1014 370/168	1661 370/195
Time to first peak (sec)	1.421	1.445	1.426	1.432	1.436
Power at first peak (MW)	5734	5451	5552	5760	5411
Time to second peak (sec)	2.0	2.0	2.0	2.0	2.0
Power at second peak (MW)	800	800*	815	840	784
Average Temp. at 3.0 sec (°K)	1070	1100*	1127	1142	1087
Maximum Temp. at 3.0 sec (°K)	2925	2989	3112	3163	2948

*Approximate

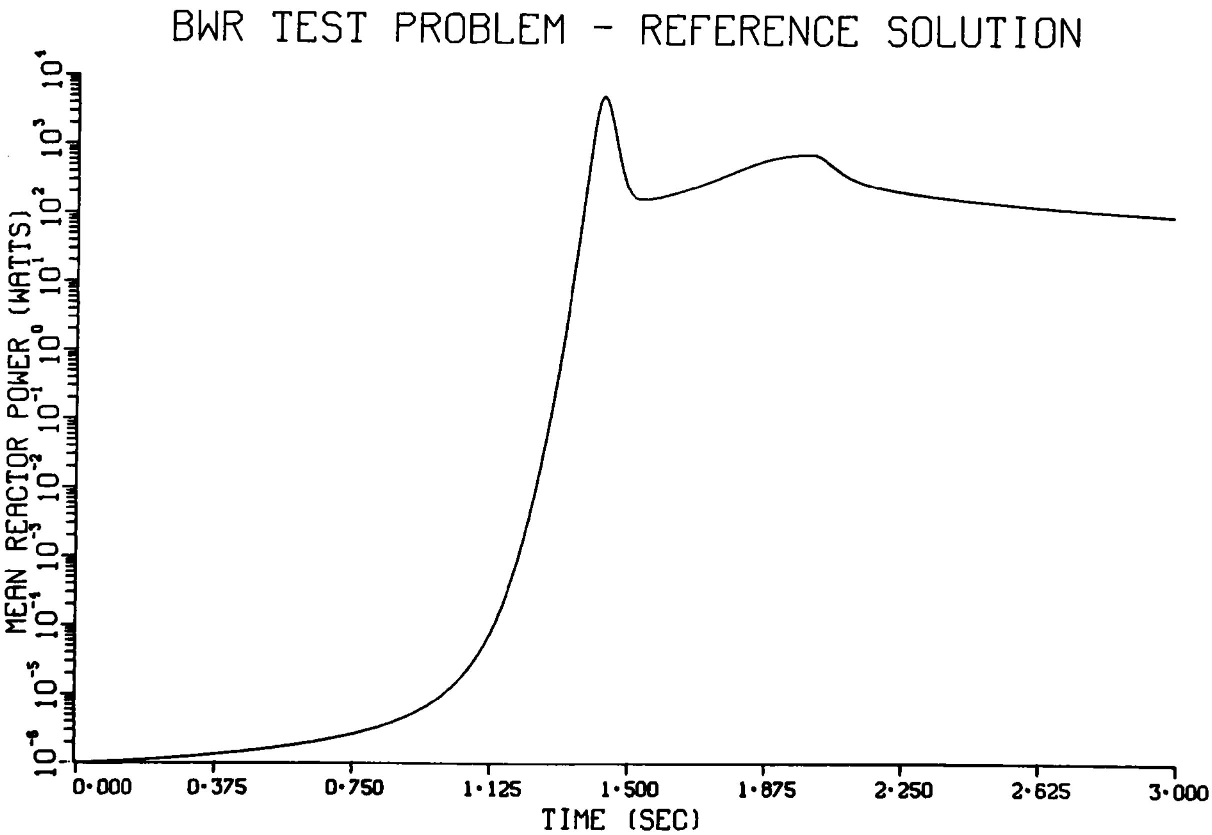

Fig. 5. Reference Solution Mean Power Versus Time
ANL Neg. No. 116-78-157

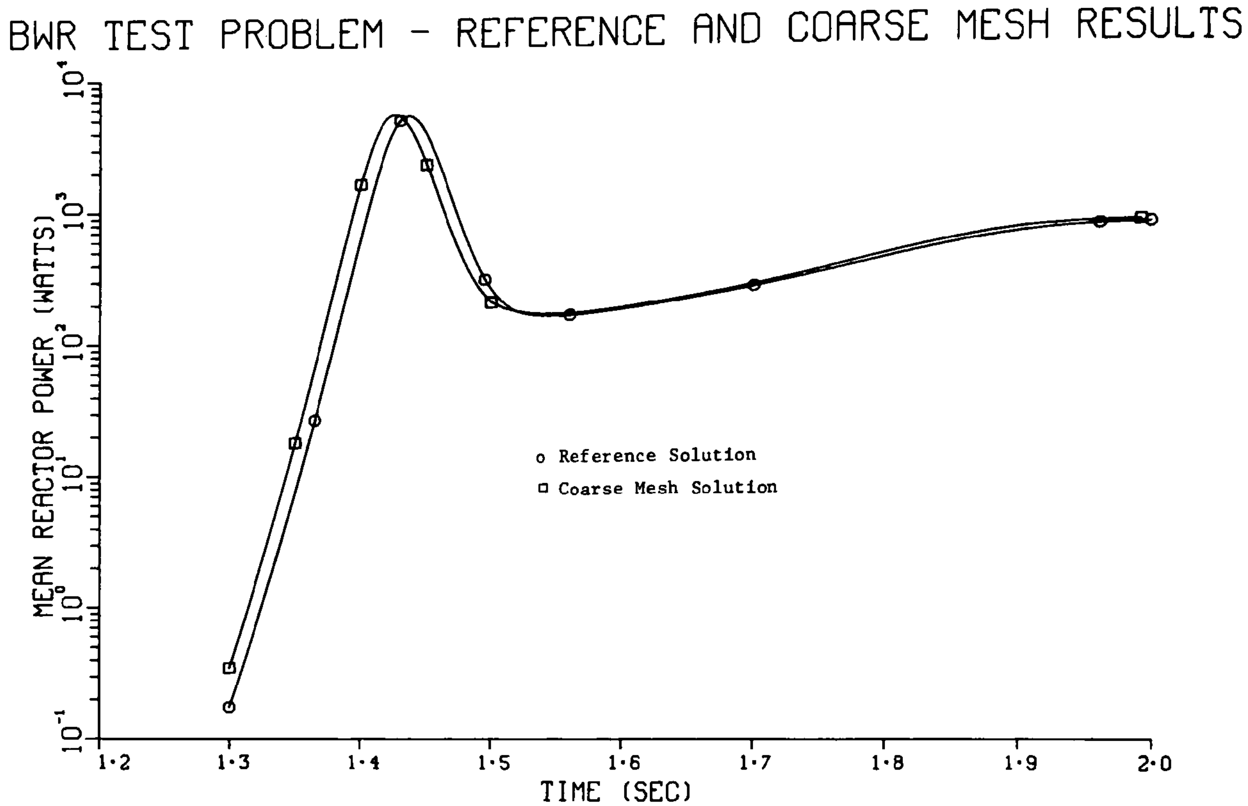

Fig. 6. Reference and Coarse Mesh Solution Mean Power Versus Time
ANL Neg. No. 116-78-156R1

times steps, MEKIN would require 57 minutes of computing time on an IBM 370/168. In addition, MEKIN uses a semi-explicit time integration method which usually requires substantially smaller time steps for equivalent accuracy than the fully-implicit method used here. Therefore, the two-step method is between 20 and 60 times more efficient than a conventional finite difference code such as MEKIN.

V. SUMMARY

A. Summary of Results

The test problem results shown in this report demonstrate the accuracy and efficiency of the methods developed here. In general, the two-step leakage method produced acceptably accurate results for all the test problems presented here. In addition, the execution times were comparable to other highly successful nodal methods which have been reported in the literature.

B. Further Developments

Up to the present time, very little work has been done towards applying nodal schemes to the analysis of fast reactors. Fast reactors have generally larger diffusion lengths; thus finite difference methods are more effective in their analysis than for LWR's. However, demands of multidimensional fast reactor analysis make investigation into the application of nodal methods potentially fruitful.

A brief study of the algebra in Appendix A demonstrates clearly why the method developed in this report is restricted to one- or two-energy groups. There are, however, several different techniques for the possible extension of this method to multigroup problems.

Equation (II.30) is a very general equation, evidenced by the fact that it was obtained from both the response matrix and the analytic solution techniques. If other, more indirect means were available for determining the matrices $[A^i_{1,2}]$ and $[B^i_{1,1}]$, the method could be extended in a straightforward manner. One possible technique would be to diagonalize the matrix $e^{[N_i]h_i}$; another possible technique is to use some form of table look-up. The diagonalization of the above matrix might prove to be difficult, since the eigenvectors and eigenvalues of $[N_i]$ would be required. Another drawback of this scheme is that the resultant equations would have more extensive coupling than that of finite difference methods. This was briefly discussed in Section II.D.

Another approach is to solve analytically the one-dimensional diffusion equation for only one group at a time. Let us rewrite Eq. (II.1) as follows:

$$- \frac{d}{dx} D_g(x) \frac{d}{dx} \phi_g(x) + \Sigma_{T_g}(x)\, \phi_g(x) = S_g(x) \tag{V.1}$$

where $S_g(x)$ contains the fissioning and scattering terms into group g. Equation (V.1) could be solved analytically using the same techniques as shown in this report, provided the functional form of $S_g(x)$ were known. It is doubtful that as simple a form as the flat or even the two-step approximations would be adequate. However, due to the success in Reference 11, a quadratic function may be sufficiently accurate. The technique for generating this quadratic is a subject of future investigation. The advantage of a scheme such as this would be that the coupling relationship between adjacent average fluxes would be the same as in conventional finite difference methods.

A number of other improvements are currently under investigation. Researchers at the Massachusetts Institute of Technology[15] are currently implementing a quadratic transverse leakage approximation as done in References 3 and 5. Such a method would be highly accurate, but may suffer in execution time. They are also investigating methods of solving the steady-state equations using Weilandt's iterations. This is being explored so that the method can be adapted to use a quasistatic treatment of the time dependence.

The similarity of the response matrix and analytic solution derivations points out the considerable promise of research into the overall relationships of the nodal methods currently being investigated. Much work has been begun by Weiss.[16] Further investigation into these subjects will doubtlessly be very fruitful.

References

1. A. F. Henry, Nuclear-Reactor Analysis (Cambridge, Mass: MIT Press), 1975.

2. J. R. Lamarsh, Nuclear Reactor Theory (Reading, Mass; Addison-Wesley), 1966.

3. H. Finnemann, F. Bennewitz, M. R. Wagner, "Interface Current Techniques for Multidimensional Reactor Calculations," Atomkernenergie, Vol. 30, No. 2, p. 123 (1977).

4. S. Langenbuch, W. Maurer, W. Werner, "Coarse-Mesh Flux-Expansion Method for the Analysis of Space-Time Effects in Large Light-Water Reactor Cores," Nucl. Sci. Eng. 63, p. 437 (1977).

5. R. Sims and A. F. Henry, "Coarse Mesh Nodal Method Based on Response Matrix Considerations," Trans. Am. Nucl. Soc. 24 (1976).

6. C. M. Kang and K. F. Hansen, "Finite Element Methods for Reactor Analysis," Nucl. Sci. Eng. 51, pp. 456-495 (1973).

7. R. A. Shober and A. F. Henry, "Nonlinear Methods for Solving the Diffusion Equation," MITNE-196, Massachusets Institute of Technology, Cambridge Mass. (November 1976).

8. R. A. Shober and A. F. Henry, "An Approximate Analytical Method for Determining Nodal Fluxes," Trans. Am. Nucl. Soc. 24, p. 192 (1976).

9. R. A. Shober, R. N. Sims, A. F. Henry, "Two Nodal Method for Solving Time-Dependent Group Diffusion Equations," Nucl. Sci. Eng. 64, p. 582 (1977).

10. Argonne Code Center: Benchmark Problem Book, ANL-7416, June 1977 (Supplement II).

11. K. Aoki and M. Tsuiki, "A New Method for the Numerical Solution of the Two-Dimensional Neutron Diffusion Equation," Nucl. Sci. Eng. 57, pp. 53-62 (1975).

12. E. L. Wachpress, "Interative Solution of Elliptic Systems," (Prentice-Hall, 1966), p. 83.

13. G. K. Kristiansen, "Investigation of the Accuracy of Centerpoint-, Cornerpoint-, and Finite Element Methods for Solution of the Neutron Diffusion Equation," RP-3-76/NEACRP-L-189.

14. R. W. Bowring, J. W. Stewart, R. A. Shober, R. N. Sims, "MEKIN: MIT-EPRI Nuclear Reactor Core Kinetics Code," CCM-1, Research Project 227, Electric Power Research Institute (September 1975).

15. A. F. Henry, private communications (1978).

16. Z. Weiss, "Some Basic Properties of the Response Matrix Equations," Nucl. Sci. Eng. 63, pp. 457-492 (1977).

APPENDIX A

CALCULATION OF MATRICES

In the derivation of the computing equations, the following matrices are required:

$$[A^i] = (\tanh[N_i]h_i/2) \qquad \text{element } (1,2)$$

$$[B^i] = (\sinh^{-1}[N_i]h_i)[N_i]h_i \qquad \text{element } (1,1)$$

$$[D^i] = -(\sinh^{-1}[N_i]h_i)h_i + [N_i]^{-1} \qquad \text{element } (1,2)$$

$$[F^i] = [N_i]^{-1}\left(\frac{1}{2}\right)(\tanh[N_i]h_i/2) \cdot \left\{[I] - \tanh[N_i]h_i/4\right\}^2 \qquad \text{element } (1,2)$$

Assume region R_i $(x_i \leq x \leq x_{i+1})$ is homogeneous. In two groups, we can write the diffusion equations:

$$\begin{bmatrix} D_1 \frac{d^2}{dx^2} - \sum_1 & \frac{1}{\lambda}\nu\sum_{f_2} \\ \sum_{r_1} & D_2 \frac{d^2}{dx^2} - \sum_2 \end{bmatrix} \begin{bmatrix} \phi_1(x) \\ \phi_2(x) \end{bmatrix} = 0 \tag{A.1}$$

where $\sum_1 = \sum_{T_1} - \frac{1}{\lambda}\nu\sum_{f_1}$

We seek particular solutions such that

$$\begin{bmatrix} \frac{d^2}{dx^2} & 0 \\ 0 & \frac{d^2}{dx^2} \end{bmatrix} \begin{bmatrix} \phi_1(x) \\ \phi_2(x) \end{bmatrix} = \begin{bmatrix} -B^2 & 0 \\ 0 & -B^2 \end{bmatrix} \begin{bmatrix} \phi_1(x) \\ \phi_2(x) \end{bmatrix} \tag{A.2}$$

We find that the numbers B^2 must be chosen such that

$$\begin{bmatrix} -D_1B^2 - \Sigma_1 & \frac{1}{\lambda}\nu\Sigma_{f_2} \\ \Sigma_{r_1} & -D_2B^2 - \Sigma_2 \end{bmatrix} \begin{bmatrix} \phi_1(x) \\ \phi_2(x) \end{bmatrix} = 0 \qquad \text{(A.3)}$$

Therefore, the determinant of the coefficient matrix in Eq. (A.3) must vanish. We find that there are two and only two values of B^2 which satisfy Eq. (A.2). These values, designated κ^2 and $-\mu^2$, are defined as:

$$\kappa^2 = -\frac{1}{2}\left(\frac{\Sigma_1}{D_1} + \frac{\Sigma_2}{D_2}\right) + \sqrt{\left(\frac{\Sigma_2}{2D_2} - \frac{\Sigma_1}{2D_1}\right)^2 + \frac{\nu\Sigma_{f_2}\Sigma_{r_i}}{\lambda D_1 D_2}} \qquad \text{(A.4)}$$

$$\mu^2 = \frac{1}{2}\left(\frac{\Sigma_1}{D_1} + \frac{\Sigma_2}{D_2}\right) + \sqrt{\left(\frac{\Sigma_2}{2D_2} - \frac{\Sigma_1}{2D_1}\right)^2 + \frac{\nu\Sigma_{f_2}\Sigma_{r_1}}{\lambda D_1 D_2}} \qquad \text{(A.5)}$$

In the special case where $\nu\Sigma_{f_2} = 0$, we arrive at the following simple expressions

$$\kappa^2 = -\frac{\Sigma_1}{D_1} \qquad \text{(A.6)}$$

$$\mu^2 = \frac{\Sigma_2}{D_2} \qquad \text{(A.7)}$$

In Eqs. (A.4) and (A.5), μ^2 is always positive, and κ^2 can be either negative or positive. If $\nu\Sigma_{f_2} = 0$, κ^2 is always negative.

Next, let us define

$$R(B^2) = \frac{\phi_2}{\phi_1} = \frac{\sum_{r_1}}{D_2B^2+\sum_2} \tag{A.8}$$

so we also define

$$\begin{aligned} R(\kappa^2) &\equiv r \\ R(-\mu^2) &\equiv s \end{aligned} \tag{A.9}$$

Therefore, the general solution to Eq. (A.1) is:

$$\begin{bmatrix} \phi_1(x) \\ \phi_2(x) \end{bmatrix} = a_1 \begin{bmatrix} 1 \\ r \end{bmatrix} \sin \kappa x + a_2 \begin{bmatrix} 1 \\ r \end{bmatrix} \cos \kappa x + a_3 \begin{bmatrix} 1 \\ s \end{bmatrix} \sinh \mu x + a_4 \begin{bmatrix} 1 \\ s \end{bmatrix} \cosh \mu x$$

or

$$\begin{bmatrix} \phi_1(x) \\ \phi_2(x) \end{bmatrix} = \begin{bmatrix} 1 & 1 \\ r & s \end{bmatrix} \begin{bmatrix} a_1 \sin \kappa x + a_2 \cos \kappa x \\ a_3 \sinh \mu x + a_4 \cosh \mu x \end{bmatrix} \tag{A.10}$$

The corresponding current vector is

$$\begin{bmatrix} J_1(x) \\ J_2(x) \end{bmatrix} = \begin{bmatrix} -D_1\frac{d}{dx} \phi_1(x) \\ -D_2\frac{d}{dx} \phi_2(x) \end{bmatrix} =$$

$$= \begin{bmatrix} -D_1 & -D_1 \\ -D_2 r & -D_2 s \end{bmatrix} \begin{bmatrix} a_1 \kappa \cos \kappa x - a_2 \kappa \sin \ x \\ a_3 \mu \cosh \mu x + a_4 \mu \sinh \mu x \end{bmatrix}$$

Therefore, write the total flux-current vector as

$$[\Phi(x)] = \text{col}\left\{ \phi_1(x), \phi_2(x), J_1(x), J_2(x) \right\}$$

$$= \begin{bmatrix} 1 & 1 & 0 & 0 \\ r & s & 0 & 0 \\ 0 & 0 & -D_1 & -D_1 \\ 0 & 0 & -D_2 r & -D_2 s \end{bmatrix} \begin{bmatrix} \sin \kappa x & \cos \kappa x & 0 & 0 \\ 0 & 0 & \sinh \mu x & \cosh \mu x \\ \kappa \cos \kappa x & -\kappa \sin \kappa x & 0 & 0 \\ 0 & 0 & \mu \cosh \mu x & \mu \sinh \mu x \end{bmatrix} \begin{bmatrix} a_1 \\ a_2 \\ a_3 \\ a_4 \end{bmatrix}$$

$$= [E]\,[F(x)]\,[A]$$

where

$$[A] = \text{col}\left\{ a_1, a_2, a_3, a_4 \right\}$$

Therefore we write the above equation as

$$[\Phi(x)] = [E]\,[F(x)]\,[A] \tag{A.11}$$

Both the matrices [E] and [F(x)] have inverses. They are

$$[E]^{-1} = \frac{1}{s-r} \begin{bmatrix} s & -1 & 0 & 0 \\ -r & 1 & 0 & 0 \\ 0 & 0 & -\frac{s}{D_1} & \frac{1}{D_2} \\ 0 & 0 & \frac{r}{D_1} & -\frac{1}{D_2} \end{bmatrix}$$

$$[F(x)]^{-1} = \begin{bmatrix} \sin \kappa x & 0 & \frac{1}{\kappa} \cos \kappa x & 0 \\ \cos \kappa x & 0 & -\frac{1}{\kappa} \sin \kappa x & 0 \\ 0 & -\sinh \mu x & 0 & \frac{1}{\mu}\cosh \mu x \\ 0 & \cosh \mu x & 0 & -\frac{1}{\mu}\sinh \mu x \end{bmatrix}$$

The coefficients in the general expansion are then given by

$$[A] = [F(x)]^{-1} [E]^{-1} [\Phi(x)] \tag{A.12}$$

If a homogeneous region extends from x_1 and x_2, we may find $[\Phi(x_1)]$ in terms of $[\Phi(x_2)]$ by applying Eq. (A.11) for $x = x_1$ and Eq. (A.12) for $x = x_2$. Thus

$$[\Phi(x_1)] = [E] [F(x_1)] [F(x_2)]^{-1} [E]^{-1} [\Phi(x_2)] \tag{A.13}$$

Defining $h = x_2 - x_1$, multiplying out and rearranging, we have $[G(h)] = [F(x_1)] [F(x_2)]^{-1}$

$$= \begin{bmatrix} \cos \kappa h & 0 & -\frac{1}{\kappa} \sin \kappa h & 0 \\ 0 & \cosh \mu h & 0 & -\frac{1}{\mu} \sinh \mu h \\ \kappa \sin \kappa h & 0 & \cosh \kappa h & 0 \\ 0 & -\mu \sinh \kappa h & 0 & \cosh \mu h \end{bmatrix}$$

Therefore

$$[\Phi(x_1)] = [E] [G(h)] [E]^{-1} [\Phi(x_2)] \tag{A.14}$$

Comparing Eq. (A.14) to Eq. (II.23), we see

$$[\Phi(x_1)] = e^{[N_i]h_i} [\Phi(x_2)]$$

so

$$e^{[N_i]h_i} = [E]\ [G(h)]\ [E]^{-1} \tag{A.15}$$

We can split Eq. (A.15) into sub-blocks:

$$e^{[N_i]h_i} = \begin{bmatrix} E_{11} & 0 \\ 0 & E_{22} \end{bmatrix} \begin{bmatrix} G_{11}(h) & G_{12}(h) \\ G_{21}(h) & G_{22}(h) \end{bmatrix} \begin{bmatrix} E_{11}^{-1} & 0 \\ 0 & E_{22}^{-1} \end{bmatrix}$$

Now, we must evaluate certain expressions. Use the identities

$$\sinh x = \frac{1}{2}(e^{x} - e^{-x})$$

we know·

$$e^{-[N_i]h_i} = [E]\ [G(-h)]\ [E]^{-1}$$

Therefore

$$\sinh [N_i]h_i = [E] \left\{ \frac{1}{2}[G(h)] - \frac{1}{2}[G(-h) \right\} [E]^{-1}$$

$$= \begin{bmatrix} E_{11} & 0 \\ 0 & E_{22} \end{bmatrix} \begin{bmatrix} 0 & 0 & -\frac{1}{\kappa}\sin \kappa h & 0 \\ 0 & 0 & 0 & -\frac{1}{\mu}\sinh \mu h \\ \kappa \sin \kappa h & 0 & 0 & 0 \\ 0 & -\mu \sinh \mu h & 0 & 0 \end{bmatrix}$$

$$\cdot \begin{bmatrix} E_{11}^{-1} & 0 \\ 0 & E_{22}^{-1} \end{bmatrix} \tag{A.16}$$

or,

$$\sinh\,[N_i]h_i = \begin{bmatrix} E_{11} & 0 \\ 0 & E_{22} \end{bmatrix} \begin{bmatrix} 0 & H_{12}(h) \\ H_{21}(h) & 0 \end{bmatrix} \begin{bmatrix} E_{11}^{-1} & 0 \\ 0 & E_{22}^{-1} \end{bmatrix} \tag{A17}$$

Next, use the identity

$$\tanh x = (e^{x} + e^{-x})^{-1}\,(e^{x} - e^{-x})$$

or

$$\tanh[N_i]h_i = \left\{[E]\left([G(h)] + [G(-h)]\right)\ [E]^{-1}\right\}^{-1}$$

$$\cdot\ \left\{[E]\left([G(h)] - [G(-h)]\right)\ [E]^{-1}\right\}$$

The inverse is

$$= [E]\left([G(h)] + [G(-h)]\right)^{-1}\ [E]^{-1}$$

or

$$\tanh[N_i]h_i = [E]\left([G(h)] + [G(-h)]^{-1}\right)[E]^{-1}$$

$$\cdot\ [E]\left([G(h)] - [G(-h)]\right)\ [E]^{-1}$$

$$= [E]\left([G(h)] + [G(-h)]^{-1}\right)$$

$$\cdot\ \left([G(h)] - [G(-h)]\right)\ [E]^{-1}$$

$$\left([G(h)] + [G(-h)]\right) = \begin{bmatrix} 2\cos\kappa h & 0 & 0 & 0 \\ 0 & 2\cosh\mu h & 0 & 0 \\ 0 & 0 & 2\cos\kappa h & 0 \\ 0 & 0 & 0 & 2\cosh\mu h \end{bmatrix}$$

Therefore

$$\left([G(h)] + [G(-h)]\right)^{-1}\left([G(h)] - [G(-h)]\right)$$

$$= \begin{bmatrix} 0 & 0 & -\frac{\tan\kappa h}{\kappa} & 0 \\ 0 & 0 & 0 & -\frac{\tanh\mu h}{\mu} \\ \kappa\tan\kappa h & 0 & 0 & 0 \\ 0 & -\mu\tanh\mu h & 0 & 0 \end{bmatrix}$$

$$= [J(h)]$$

so

$$\tanh[N_i]h_i = \begin{bmatrix} E_{11} & 0 \\ 0 & E_{22} \end{bmatrix} \begin{bmatrix} 0 & J_{12}(h) \\ J_{21}(h) & 0 \end{bmatrix} \begin{bmatrix} E_{11}^{-1} & 0 \\ 0 & E_{22}^{-1} \end{bmatrix} \tag{A.18}$$

From relationships Eq. (A.17) and (A.18), we can determine the required matrices.

1) $\tanh[N_i]h_i/2$ element 1,2

$$= \begin{bmatrix} E_{11} & 0 \\ 0 & E_{22} \end{bmatrix} \begin{bmatrix} 0 & J_{12}(h/2) \\ J_{21}(h/2) & 0 \end{bmatrix} \begin{bmatrix} E_{11}^{-1} & 0 \\ 0 & E_{22}^{-1} \end{bmatrix}$$

The 1,2 element is

$$= [E_{11}]\ [J_{12}(h/2)]\ [E_{22}^{-1}]$$

Let $[A^i_{1,2}]$ = the 1,2 element of $\tanh[N_i]h_i/2$ then

$$[A^i_{1,2}] = \left(\frac{1}{s-r}\right) \begin{bmatrix} \left(\dfrac{s \tan \kappa h/2}{\kappa D_1} - \dfrac{r \tanh \mu h/2}{\mu D_1}\right) & \left(-\dfrac{\tan \kappa h/2}{\kappa D_2} + \dfrac{\tanh \mu h/2}{\mu D_2}\right) \\ \left(\dfrac{rs \tan \kappa h/2}{\kappa D_1} - \dfrac{rs \tanh \mu h/2}{\mu D_1}\right) & \left(-\dfrac{r \tan \kappa h/2}{\kappa D_2} + \dfrac{s \tanh \mu h/2}{\mu D_2}\right) \end{bmatrix}$$

2) $(\sinh^{-1}[N_i]h_i)[N_i]h_i$ element 1,1 denote this as $[B^i_{1,1}]$.

$$[B^i] = \begin{bmatrix} E_{11} & 0 \\ 0 & E_{22} \end{bmatrix} \begin{bmatrix} 0 & H_{21}^{-1}(h) \\ H_{12}^{-1}(h) & 0 \end{bmatrix} \begin{bmatrix} E_{11}^{-1} & 0 \\ 0 & E_{22}^{-1} \end{bmatrix} \begin{bmatrix} 0 & N_{12} \\ N_{21} & 0 \end{bmatrix}$$

$$[B^i_{1,1}] = [E_{11}]\ [H_{21}^{-1}(h)]\ [E_{22}^{-1}]\ [N_{21}]$$

when multiplied out, this becomes

$$[B^i_{1,1}] = \left(\frac{h_i}{s-r}\right) \begin{bmatrix} (\kappa s \csc \kappa h - \mu r \operatorname{csch} \mu h) \\ (sr\kappa \csc \kappa h - sr\,\mu \operatorname{csch} \mu h) \end{bmatrix}$$

$$\begin{matrix} (-\ \kappa\ \csc \kappa h + \mu\ \mathrm{csch}\ \mu h) \\ (-\ \kappa r\ \csc \kappa h + \mu s\ \mathrm{csch}\ \mu h) \end{matrix}\Bigg] \qquad \text{(A.20)}$$

3) $$[D^i] = -(\sinh^{-1}[N_i]h_i)h_i + [N_i]^{-1} \qquad \text{(element 1,2)}$$

$$[D^i] = -\begin{bmatrix} E_{11} & 0 \\ 0 & E_{22} \end{bmatrix}\begin{bmatrix} 0 & H_{21}^{-1}(h) \\ H_{12}^{-1}(h) & 0 \end{bmatrix}\begin{bmatrix} E_{11}^{-1} & 0 \\ 0 & E_{22}^{-1} \end{bmatrix} h_i$$

$$+ \begin{bmatrix} 0 & N_{21}^{-1} \\ N_{12}^{-1} & 0 \end{bmatrix}$$

$$[D^i_{1,2}] = -[E_{11}]\ [H_{21}^{-1}(h)]\ [E_{22}^{-1}]\ h_i + [N_{21}]^{-1}$$

use the relationship

$$[N_{21}]^{-1} = \begin{bmatrix} \frac{1}{\kappa^2} & -\frac{1}{\mu^2} \\ \frac{r}{\kappa^2} & -\frac{s}{\mu^2} \end{bmatrix} [E_{22}]^{-1}$$

so

$$[D^i_{1,2}] = \left\{ -h_i[E_{11}]\ [H_{21}^{-1}(h)] + \begin{bmatrix} \frac{1}{\kappa^2} & -\frac{1}{\mu^2} \\ \frac{r}{\kappa^2} & -\frac{s}{\mu^2} \end{bmatrix} \right\} \cdot [E_{22}]^{-1}$$

when this is expressed, it becomes

$$[D^i_{1,2}] = \frac{h_i}{s-r}\begin{bmatrix} -\dfrac{\csc \kappa h}{\kappa} & \dfrac{\operatorname{csch} \mu h}{\mu} \\ -\dfrac{r \csc \kappa h}{\kappa} & \dfrac{s \operatorname{csch} \mu h}{\mu} \end{bmatrix}\begin{bmatrix} -\dfrac{s}{D_1} & \dfrac{1}{D_2} \\ \dfrac{r}{D_1} & -\dfrac{1}{D_2} \end{bmatrix}$$

$$+ \frac{1}{s-r}\begin{bmatrix} \dfrac{1}{\kappa^2} & -\dfrac{1}{\mu^2} \\ \dfrac{r}{\kappa^2} & -\dfrac{s}{\mu^2} \end{bmatrix}\begin{bmatrix} -\dfrac{s}{D_1} & \dfrac{1}{D_2} \\ \dfrac{r}{D_1} & -\dfrac{1}{D_2} \end{bmatrix} \tag{A.21}$$

4) $$[F^i] = [N]^{-1}\left(\frac{1}{2}\right)\left(\tanh[N_i]h_i/2\right) \left\{[I] - \tanh[N_i]h_i/4\right\}^2$$

element (1,2)

$$[F^i] = \frac{1}{2}\begin{bmatrix} 0 & N^{-1}_{21} \\ N^{-1}_{12} & 0 \end{bmatrix}\begin{bmatrix} E_{11} & 0 \\ 0 & E_{22} \end{bmatrix}\begin{bmatrix} 0 & J_{1,2}(h/2) \\ J_{2,1}(h/2) & 0 \end{bmatrix}$$

$$\cdot \begin{bmatrix} 1 & -J_{1,2}(h/4) \\ -J_{2,1}(h/4) & 1 \end{bmatrix}\begin{bmatrix} 1 & -J_{1,2}(h/4) \\ -J_{2,1}(h/4) & 0 \end{bmatrix}\begin{bmatrix} E^{-1}_{11} & 0 \\ 0 & E^{-1}_{22} \end{bmatrix}$$

Element 1,2

$$[F^i_{1,2}] = [N_{2,1}]^{-1}\ [E_{2,2}]\ [J_{2,1}(h/2)]\ [J_{1,2}(h/4)]\ [E_{22}]^{-1}$$

writing out this matrix and defining

$$P_1 = \tan \kappa \frac{h}{2} \tan \kappa \frac{h}{4}$$

$$P_2 = \tanh \mu \frac{h}{2} \tanh \mu \frac{h}{4}$$

$$[F^i_{1,2}] = \frac{1}{s-r} \begin{bmatrix} \frac{sP_1}{D_1\kappa^2} - \frac{rP_2}{D_1\mu^2} & -\frac{P_1}{D_2\kappa^2} + \frac{P_2}{D_2\mu^2} \\ \\ \frac{rsP_1}{D_1\kappa^2} - \frac{rsP_2}{D_1\mu^2} & -\frac{rP_1}{D_2\kappa^2} + \frac{sP_2}{D_2\mu^2} \end{bmatrix} \qquad \text{(A.22)}$$

(note if K = iK (imaginary),

$$P_1 = -(\tanh \kappa \frac{h}{2}) (\tanh \kappa \frac{h}{4}))$$

Next, these formulas have special forms in the reflector. Note if $\nu\Sigma_{f_2} = 0$, then $S\to\infty$. So we evaluate Eqs. (A.19-A.22) by using L'Hopital's rule.

$$[A^i_{1,2}] = \begin{bmatrix} \frac{\tan \kappa \frac{h}{2}}{\kappa D_1} & 0 \\ \\ \frac{r \tan \kappa \frac{h}{2}}{\kappa D_1} - \frac{r \tanh \mu \frac{h}{2}}{\mu D_1} & \frac{\tanh \mu \frac{h}{2}}{\mu D_2} \end{bmatrix} \qquad \text{(A.23)}$$

$$[B^i_{1,1}] = h_i \begin{bmatrix} \kappa \csc \kappa h & 0 \\ \\ (r\kappa \csc \kappa h - r\mu \operatorname{csch} \mu h) & (\mu \operatorname{csch} \mu h) \end{bmatrix} \qquad \text{(A.24)}$$

$$[D^i_{1,2}] = \begin{bmatrix} \dfrac{h \csc \kappa h}{D_1 \kappa} & 0 \\ \dfrac{hr \csc \kappa h}{D_1 \kappa} + \dfrac{hr \operatorname{csch} \mu h}{D_1 \mu} & -\dfrac{h \operatorname{csch} \mu h}{D_2 \mu} \end{bmatrix}$$

$$+ \begin{bmatrix} -\dfrac{1}{D_1 \kappa} & 0 \\ -\dfrac{r}{D_1 \kappa^2} + \dfrac{r}{D_1 \mu^2} & \dfrac{1}{D_2 \mu^2} \end{bmatrix} \tag{A.25}$$

$$[F^i_{1,2}] = \begin{bmatrix} \dfrac{P_1}{D_1 \kappa^2} & C \\ \dfrac{rP_1}{D_1 \kappa^2} - \dfrac{rP_2}{D_1 \mu^2} & \dfrac{P_2}{D_2 \mu^2} \end{bmatrix} \tag{A.26}$$

Next, I need to evaluate these expressions for the one-group case. The following results are obtained

	κ real	κ imaginary
$[A_{1,2}]$ =	$\dfrac{1}{DK} \tan \kappa \dfrac{h}{2}$,	$\dfrac{1}{D\kappa} \tanh \kappa \dfrac{h}{2}$
$[B_{1,1}]$ =	$\kappa h \csc \kappa h$	$\kappa h \operatorname{csch} \kappa h$
$[D_{1,2}]$ =	$\dfrac{h\csc \kappa h}{D\kappa} - \dfrac{1}{D\kappa^2}$	$-\dfrac{h \operatorname{csch} \kappa h}{D\kappa} + \dfrac{1}{D\kappa^2}$
$[F_{1,2}]$ =	$\Sigma^{-1} \left\{ \sec \kappa \dfrac{h}{2} - 1 \right\}$	$\Sigma^{-1} \left\{ \operatorname{sech} \kappa \dfrac{h}{2} - 1 \right\}$

where

$$\kappa^2 = -\frac{\Sigma}{D}$$

and

$$\Sigma = \Sigma_T - \frac{1}{\lambda}\nu\Sigma_f .$$

APPENDIX B

RESULTS OF BWR TEST PROBLEM

BWR TEST PROBLEM - REFERENCE SOLUTION

NORMALIZED ASSEMBLY POWERS AT T= 0.0

MEAN POWER DENSITY= 0.9999985E-06 AVERAGE FUEL TEMPERATURE= 0.300000E 03

9	0.9230 300.	0.8666 300.	0.8266 300.	0.8532 300.	0.9333 300.	0.9727 300.	0.8478 300.	0.0 300.	0.0 300.
8	1.4796 300.	1.2805 300.	1.1720 300.	1.2210 300.	1.4229 300.	1.6806 300.	1.6234 300.	1.3319 300.	0.0 300.
7	1.6611 300.	1.1494 300.	0.9656 300.	1.0215 300.	1.3390 300.	2.0541 300.	2.1649 300.	1.6234 300.	0.8478 300.
6	1.3854 300.	0.9387 300.	0.7817 300.	0.8425 300.	1.1516 300.	1.8543 300.	2.0541 300.	1.6806 300.	0.9727 300.
5	0.7891 300.	0.6702 300.	0.6178 300.	0.6780 300.	0.8646 300.	1.1516 300.	1.3390 300.	1.4229 300.	0.9333 300.
4	0.5110 300.	0.4900 300.	0.4919 300.	0.5524 300.	0.6780 300.	0.8425 300.	1.0215 300.	1.2210 300.	0.8532 300.
3	0.4123 300.	0.4063 300.	0.4238 300.	0.4919 300.	0.6178 300.	0.7817 300.	0.9656 300.	1.1720 300.	0.8266 300.
2	0.4395 300.	0.3991 300.	0.4063 300.	0.4900 300.	0.6702 300.	0.9387 300.	1.1493 300.	1.2805 300.	0.8666 300.
1	0.6118 300.	0.4395 300.	0.4123 300.	0.5110 300.	0.7891 300.	1.3854 300.	1.6611 300.	1.4796 300.	0.9230 300.
	1	2	3	4	5	6	7	8	9

Fig. B.1. BWR Test Problem **Results** - Reference Solution
ANL Neg. No. 116-78-176

BWR TEST PROBLEM - REFERENCE SOLUTION

NORMALIZED ASSEMBLY POWERS AT T= 0.400E 00

MEAN POWER DENSITY= 0.1386163E-05 AVERAGE FUEL TEMPERATURE= 0.300000E 03

9	0.8455 300.	0.8022 300.	0.7823 300.	0.8324 300.	0.9389 300.	1.0049 300.	0.8977 300.	0.0 300.	0.0 300.
8	1.3541 300.	1.1842 300.	1.1095 300.	1.1942 300.	1.4387 300.	1.7494 300.	1.7424 300.	1.4839 300.	0.0 300.
7	1.5187 300.	1.0615 300.	0.9145 300.	1.0024 300.	1.3624 300.	2.1535 300.	2.3526 300.	1.8911 300.	1.0264 300.
6	1.2660 300.	0.8665 300.	0.7403 300.	0.8274 300.	1.1727 300.	1.9446 300.	2.2314 300.	1.9498 300.	1.1617 300.
5	0.7214 300.	0.6190 300.	0.5842 300.	0.6623 300.	0.8722 300.	1.1937 300.	1.4255 300.	1.5533 300.	1.0324 300.
4	0.4668 300.	0.4520 300.	0.4628 300.	0.5332 300.	0.6705 300.	0.8502 300.	1.0475 300.	1.2650 300.	0.8889 300.
3	0.3753 300.	0.3730 300.	0.3953 300.	0.4674 300.	0.5962 300.	0.7631 300.	0.9512 300.	1.1613 300.	0.8218 300.
2	0.3979 300.	0.3641 300.	0.3756 300.	0.4595 300.	0.6345 300.	0.8936 300.	1.0994 300.	1.2304 300.	0.8351 300.
1	0.5520 300.	0.3991 300.	0.3793 300.	0.4760 300.	0.7409 300.	1.3055 300.	1.5700 300.	1.4026 300.	0.8770 300.
	1	2	3	4	5	6	7	8	9

Fig. B.1. (Contd) ANL Neg. No. 116-78-177

BWR TEST PROBLEM - REFERENCE SOLUTION

NORMALIZED ASSEMBLY POWERS AT T= 0.800E 00

MEAN POWER DENSITY= 0.3098074E-05 AVERAGE FUEL TEMPERATURE= 0.300000E 03

9	0.7351 300.	0.7104 300.	0.7192 300.	0.8027 300.	0.9466 300.	1.0504 300.	0.9685 300.	0.0 300.	0.0 300.
8	1.1754 300.	1.0470 300.	1.0204 300.	1.1558 300.	1.4608 300.	1.8469 300.	1.9113 300.	1.7003 300.	0.0 300.
7	1.3157 300.	0.9362 300.	0.8417 300.	0.9750 300.	1.3954 300.	2.2942 300.	2.6185 300.	2.2726 300.	1.2857 300.
6	1.0961 300.	0.7637 300.	0.6814 300.	0.8057 300.	1.2025 300.	2.0724 300.	2.4823 300.	2.3325 300.	1.4349 300.
5	0.6250 300.	0.5460 300.	0.5363 300.	0.6399 300.	0.8827 300.	1.2533 300,	1.5479 300.	1.7385 300.	1.1741 300.
4	0.4040 300.	0.3979 300.	0.4215 300.	0.5059 300.	0.6599 300.	0.8609 300.	1.0842 300.	1.3278 300.	0.9398 300.
3	0.3227 300.	0.3256 300.	0.3548 300.	0.4326 300.	0.5655 300.	0.7368 300.	0.9307 300.	1.1462 300.	0.8151 300.
2	0.3387 300.	0.3141 300.	0.3321 300.	0.4161 300.	0.5837 300.	0.8294 300.	1.0283 300.	1.1593 300.	0.7904 300.
1	0.4670 300.	0.3416 300.	0.3323 300.	0.4262 300.	0.6723 300.	1.1919 300.	1.4404 300.	1.2933 300.	0.8115 300.
	1	2	3	4	5	6	7	8	9

Fig. B.1. (Contd) ANL Neg. No. 116-78-169

BWR TEST PROBLEM - REFERENCE SOLUTION

NORMALIZED ASSEMBLY POWERS AT T= 0.120E 01

MEAN POWER DENSITY= 0.7529620E-03 AVERAGE FUEL TEMPERATURE= 0.300000E 03

9	0.5968 300.	0.5944 300.	0.6372 300.	0.7600 300.	0.9489 300.	1.0999 300.	1.0520 300.	0.0 300.	0.0 300.
8	0.9522 300.	0.8744 300.	0.9054 300.	1.1010 300.	1.4786 300.	1.9585 300.	2.1189 300.	1.9773 300.	0.0 300.
7	1.0626 300.	0.7795 300.	0.7485 300.	0.9359 300.	1.4287 300.	2.4595 300.	2.9525 300.	2.7830 300.	1.6430 300.
6	0.8846 300.	0.6355 300.	0.6066 300.	0.7753 300.	1.2340 300.	2.2245 300.	2.7997 300.	2.8459 300.	1.8104 300.
5	0.5058 300.	0.4556 300.	0.4760 300.	0.6099 300.	0.8924 300.	1.3244 300.	1.7023 300.	1.9795 300.	1.3610 300.
4	0.3268 300.	0.3312 300.	0.3698 300.	0.4707 300.	0.6445 300.	0.8720 300.	1.1288 300.	1.4059 300.	1.0037 300.
3	0.2585 300.	0.2676 300.	0.3046 300.	0.3886 300.	0.5257 300.	0.7014 300.	0.9021 300.	1.1234 300.	0.8036 300.
2	0.2668 300.	0.2533 300.	0.2783 300.	0.3615 300.	0.5187 300.	0.7458 300.	0.9349 300.	1.0647 300.	0.7302 300.
1	0.3636 300.	0.2717 300.	0.2744 300.	0.3638 300.	0.5843 300.	1.0439 300.	1.2704 300.	1.1494 300.	0.7248 300.
	1	2	3	4	5	6	7	8	9

Fig. B.1. (Contd) ANL Neg. No. 116-78-170

BWR TEST PROBLEM - REFERENCE SOLUTION

NORMALIZED ASSEMBLY POWERS AT T= 0.140E 01

MEAN POWER DENSITY= 0.6423091E 03 AVERAGE FUEL TEMPERATURE= 0.308396E 03

9	0.5406	0.5459	0.6000	0.7358	0.9403	1.1102	1.0793	0.0	0.0
	305.	305.	305.	306.	308.	309.	309.	300.	300.
8	0.8621	0.8030	0.8540	1.0697	1.4723	1.9894	2.1977	2.0984	0.0
	307.	307.	307.	309.	312.	317.	318.	318.	300.
7	0.9608	0.7155	0.7076	0.9133	1.4309	2.5115	3.0894	3.0349	1.8286
	308.	306.	306.	308.	312.	321.	326.	325.	315.
6	0.8003	0.5837	0.5744	0.7583	1.2384	2.2750	2.9332	3.1019	2.0057
	307.	305.	305.	306.	310.	319.	325.	326.	317.
5	0.4591	0.4196	0.4507	0.5948	0.8914	1.3482	1.7663	2.0898	1.4498
	304.	304.	304.	305.	307.	311.	315.	318.	312.
4	0.2972	0.3051	0.3487	0.4548	0.6354	0.8733	1.1449	1.4373	1.0302
	302.	303.	303.	304.	305.	307.	310.	312.	309.
3	0.2344	0.2454	0.2847	0.3700	0.5075	0.6842	0.8868	1.1096	0.7956
	302.	302.	302.	303.	304.	306.	307.	309.	307.
2	0.2403	0.2304	0.2574	0.3390	0.4904	0.7082	0.8918	1.0199	0.7011
	302.	302.	302.	303.	304.	306.	307.	309.	306.
1	0.3255	0.2456	0.2520	0.3382	0.5464	0.9776	1.1929	1.0833	0.6845
	303.	302.	302.	303.	305.	308.	310.	309.	306.
	1	2	3	4	5	6	7	8	9

Fig. B.1. (Contd) ANL Neg. No. 116-78-167

BWR TEST PROBLEM - REFERENCE SOLUTION

NORMALIZED ASSEMBLY POWERS AT T= 0.200E 01

MEAN POWER DENSITY= 0.7841052E 03 AVERAGE FUEL TEMPERATURE= 0.840528E 03

9	0.4640	0.4744	0.5333	0.6716	0.8827	1.0770	1.0938	0.0	0.0
	591.	593.	619.	688.	795.	886.	877.	300.	300.
8	0.7361	0.6941	0.7561	0.9740	1.3822	1.9396	2.2670	2.3378	0.0
	763.	729.	753.	862.	1072.	1348.	1477.	1456.	300.
7	0.8212	0.6180	0.6271	0.8348	1.3535	2.4781	3.2633	3.6350	2.3535
	817.	683.	674.	779.	1050.	1627.	1967.	2014.	1364.
6	0.6878	0.5072	0.5127	0.6984	1.1799	2.2585	3.1125	3.7090	2.5429
	732.	613.	605.	699.	951.	1505.	1886.	2051.	1460.
5	0.3985	0.3690	0.4061	0.5509	0.8494	1.3301	1.8314	2.2927	1.6524
	549.	526.	541.	615.	770.	1015.	1250.	1447.	1108.
4	0.2627	0.2725	0.3169	0.4215	0.6009	0.8460	1.1422	1.4745	1.0809
	462.	466.	488.	543.	637.	764.	913.	1077.	862.
3	0.2113	0.2223	0.2600	0.3408	0.4717	0.6429	0.8457	1.0749	0.7822
	430.	435.	455.	499.	571.	665.	774.	896.	730.
2	0.2199	0.2107	0.2351	0.3091	0.4461	0.6441	0.8151	0.9419	0.6552
	435.	428.	441.	484.	564.	679.	777.	847.	678.
1	0.3004	0.2256	0.2299	0.3061	0.4909	0.8760	1.0693	0.9756	0.6225
	485.	438.	439.	484.	595.	825.	940.	881.	668.
	1	2	3	4	5	6	7	8	9

Fig. B.1. (Contd) ANL Neg. No. 116-78-168

BWR TEST PROBLEM - REFERENCE SOLUTION

NORMALIZED ASSEMBLY POWERS AT T= 0.300E 01

MEAN POWER DENSITY= 0.9617526E 02 AVERAGE FUEL TEMPERATURE= 0.108732E 04

9	0.5056 711.	0.5094 714.	0.5575 754.	0.6823 855.	0.8773 1012.	1.0555 1149.	1.0631 1143.	0.0 300.	0.0 300.
8	0.8025 954.	0.7455 907.	0.7892 943.	0.9862 1104.	1.3673 1411.	1.8911 1821.	2.1913 2027.	2.2499 2022.	0.0 300.
7	0.8971 1030.	0.6650 841.	0.6542 833.	0.8427 986.	1.3334 1381.	2.4088 2230.	3.1457 2757.	3.4880 2892.	2.2578 1933.
6	0.7531 910.	0.5471 743.	0.5357 734.	0.7056 872.	1.1631 1240.	2.1967 2055.	3.0024 2640.	3.5621 2948.	2.4424 2075.
5	0.4375 652.	0.3992 621.	0.4266 643.	0.5605 752.	0.8438 979.	1.3018 1339.	1.7770 1695.	2.2169 2003.	1.5982 1509.
4	0.2905 531.	0.2970 536.	0.3364 568.	0.4349 648.	0.6065 786.	0.8414 972.	1.1262 1193.	1.4491 1438.	1.0623 1127.
3	0.2366 485.	0.2454 493.	0.2802 522.	0.3583 586.	0.4867 690.	0.6551 825.	0.8548 984.	1.0825 1162.	0.7871 924.
2	0.2498 493.	0.2360 483.	0.2572 502.	0.3306 563.	0.4699 677.	0.6722 842.	0.8451 982.	0.9722 1083.	0.6753 842.
1	0.3440 564.	0.2551 497.	0.2538 499.	0.3304 563.	0.5221 720.	0.9249 1048.	1.1234 1211.	1.0211 1127.	0.6507 825.
	1	2	3	4	5	6	7	8	9

Fig. B.1. (Contd) ANL Neg. No. 116-78-162

BWR TEST PROBLEM - COARSE MESH SOLUTION - TWO-STEP LEAKAGE

NORMALIZED ASSEMBLY POWERS AT T= 0.0

MEAN POWER DENSITY= 0.9999976E-06 AVERAGE FUEL TEMPERATURE= 0.300000E 03

9	0.9189 300.	0.8649 300.	0.8260 300.	0.8544 300.	0.9364 300.	0.9772 300.	0.8481 300.	0.0 300.	0.0 300.
8	1.4755 300.	1.2788 300.	1.1687 300.	1.2200 300.	1.4283 300.	1.6859 300.	1.6310 300.	1.3362 300.	0.0 300.
7	1.6633 300.	1.1447 300.	0.9617 300.	1.0187 300.	1.3383 300.	2.0654 300.	2.1791 300.	1.6310 300.	0.8481 300.
6	1.3862 300.	0.9354 300.	0.7786 300.	0.8400 300.	1.1503 300.	1.8622 300.	2.0654 300.	1.6859 300.	0.9772 300.
5	0.7852 300.	0.6699 300.	0.6168 300.	0.6775 300.	0.8663 300.	1.1503 300.	1.3383 300.	1.4283 300.	0.9364 300.
4	0.5079 300.	0.4887 300.	0.4918 300.	0.5527 300.	0.6775 300.	0.8400 300.	1.0187 300.	1.2200 300.	0.8544 300.
3	0.4097 300.	0.4048 300.	0.4234 300.	0.4918 300.	0.6168 300.	0.7786 300.	0.9617 300.	1.1687 300.	0.8260 300.
2	0.4368 300.	0.3980 300.	0.4048 300.	0.4887 300.	0.6699 300.	0.9354 300.	1.1447 300.	1.2788 300.	0.8649 300.
1	0.6111 300.	0.4368 300.	0.4097 300.	0.5079 300.	0.7852 300.	1.3862 300.	1.6633 300.	1.4755 300.	0.9189 300.
	1	2	3	4	5	6	7	8	9

Fig. B.2. BWR Test Problem Results - Coarse Mesh Two-Step Leakage Solution ANL Neg. No. 116-78-161

BWR TEST PROBLEM - COARSE MESH SOLUTION - TWO-STEP LEAKAGE

NORMALIZED ASSEMBLY POWERS AT T= 0.4000E 00

MEAN POWER DENSITY= 0.1390311E-05 AVERAGE FUEL TEMPERATURE= 0.300000E 03

9	0.8406 300.	0.7997 300.	0.7812 300.	0.8336 300.	0.9425 300.	1.0105 300.	0.8986 300.	0.0 300.	0.0 300.
8	1.3484 300.	1.1811 300.	1.1056 300.	1.1930 300.	1.4447 300.	1.7562 300.	1.7522 300.	1.4898 300.	0.0 300.
7	1.5185 300.	1.0559 300.	0.9101 300.	0.9994 300.	1.3619 300.	2.1661 300.	2.3699 300.	1.9034 300.	1.0286 300.
6	1.2652 300.	0.8625 300.	0.7369 300.	0.8247 300.	1.1715 300.	1.9534 300.	2.2452 300.	1.9595 300.	1.1693 300.
5	0.7170 300.	0.6181 300.	0.5828 300.	0.6617 300.	0.8740 300.	1.1929 300.	1.4255 300.	1.5600 300.	1.0368 300.
4	0.4635 300.	0.4504 300.	0.4625 300.	0.5334 300.	0.6701 300.	0.8477 300.	1.0446 300.	1.2637 300.	0.8901 300.
3	0.3725 300.	0.3713 300.	0.3947 300.	0.4671 300.	0.5949 300.	0.7597 300.	0.9467 300.	1.1572 300.	0.8206 300.
2	0.3950 300.	0.3626 300.	0.3740 300.	0.4579 300.	0.6336 300.	0.8895 300.	1.0937 300.	1.2271 300.	0.8324 300.
1	0.5507 300.	0.3963 300.	0.3764 300.	0.4726 300.	0.7364 300.	1.3047 300.	1.5699 300.	1.3968 300.	0.8718 300.
	1	2	3	4	5	6	7	8	9

Fig. B.2. (Contd) ANL Neg. No. 116-78-163

BWR TEST PROBLEM - COARSE MESH SOLUTION - TWO-STEP LEAKAGE

NORMALIZED ASSEMBLY POWERS AT T= 0.8000E 00

MEAN POWER DENSITY= 0.3165021E-05 AVERAGE FUEL TEMPERATURE= 0.300000E 03

9	0.7287 300.	0.7065 300.	0.7173 300.	0.8038 300.	0.9511 300.	1.0578 300.	0.9707 300.	0.0 300.	0.0 300.
8	1.1670 300.	1.0416 300.	1.0153 300.	1.1544 300.	1.4678 300.	1.8561 300.	1.9249 300.	1.7089 300.	0.0 300.
7	1.3119 300.	0.9292 300.	0.8364 300.	0.9716 300.	1.3951 300.	2.3089 300.	2.6410 300.	2.2927 300.	1.2916 300.
6	1.0924 300.	0.7584 300.	0.6773 300.	0.8026 300.	1.2013 300.	2.0827 300.	2.5003 300.	2.3496 300.	1.4477 300.
5	0.6196 300.	0.5440 300.	0.5343 300.	0.6390 300.	0.8848 300.	1.2533 300.	1.5494 300.	1.7474 300.	1.1806 300.
4	0.4001 300.	0.3957 300.	0.4205 300.	0.5058 300.	0.6594 300.	0.8586 300.	1.0814 300.	1.3261 300.	0.9410 300.
3	0.3195 300.	0.3235 300.	0.3537 300.	0.4318 300.	0.5638 300.	0.7328 300.	0.9253 300.	1.1406 300.	0.8129 300.
2	0.3354 300.	0.3122 300.	0.3300 300.	0.4139 300.	0.5818 300.	0.8240 300.	1.0209 300.	1.1535 300.	0.7861 300.
1	0.4646 300.	0.3384 300.	0.3291 300.	0.4223 300.	0.6667 300.	1.1883 300.	1.4367 300.	1.2844 300.	0.8046 300.
	1	2	3	4	5	6	7	8	9

Fig. B.2. (Contd) ANL Neg. No. 116-78-164

BWR TEST PROBLEM - COARSE MESH SOLUTION - TWO-STEP LEAKAGE

NORMALIZED ASSEMBLY POWERS AT T= 0.1200E 01

MEAN POWER DENSITY= 0.1065549E-02 AVERAGE FUEL TEMPERATURE= 0.300000E 03

9	0.5901 300.	0.5899 300.	0.6347 300.	0.7610 300.	0.9538 300.	1.1085 300.	1.0546 300.	0.0 300.	0.0 300.
8	0.9430 300.	0.8679 300.	0.8997 300.	1.0992 300.	1.4858 300.	1.9688 300.	2.1350 300.	1.9868 300.	0.0 300.
7	1.0569 300.	0.7721 300.	0.7430 300.	0.9320 300.	1.4276 300.	2.4738 300.	2.9776 300.	2.8106 300.	1.6523 300.
6	0.8797 300.	0.6300 300.	0.6023 300.	0.7718 300.	1.2319 300.	2.2340 300.	2.8195 300.	2.8698 300.	1.8285 300.
5	0.5005 300.	0.4531 300.	0.4738 300.	0.6088 300.	0.8944 300.	1.3245 300.	1.7043 300.	1.9891 300.	1.3686 300.
4	0.3232 300.	0.3289 300.	0.3687 300.	0.4704 300.	0.6440 300.	0.8697 300.	1.1254 300.	1.4026 300.	1.0041 300.
3	0.2557 300.	0.2656 300.	0.3034 300.	0.3876 300.	0.5236 300.	0.6971 300.	0.8958 300.	1.1159 300.	0.7999 300.
2	0.2640 300.	0.2514 300.	0.2763 300.	0.3592 300.	0.5162 300.	0.7396 300.	0.9261 300.	1.0564 300.	0.7243 300.
1	0.3613 300.	0.2688 300.	0.2714 300.	0.3598 300.	0.5784 300.	1.0383 300.	1.2636 300.	1.1380 300.	0.7164 300.
	1	2	3	4	5	6	7	8	9

Fig. B.2. (Contd) ANL Neg. No. 116-78-172

BWR TEST PROBLEM - COARSE MESH SOLUTION - TWO-STEP LEAKAGE

NORMALIZED ASSEMBLY POWERS AT T= 0.1400E 01

MEAN POWER DENSITY= 0.1641903E 04 AVERAGE FUEL TEMPERATURE= 0.322066E 03

9	0.5383 312.	0.5448 312.	0.5997 313.	0.7374 316.	0.9441 321.	1.1167 325.	1.0791 324.	0.0 300.	0.0 300.
8	0.8596 319.	0.8014 318.	0.8512 319.	1.0681 324.	1.4767 333.	1.9937 344.	2.2067 349.	2.1007 346.	0.0 300.
7	0.9625 321.	0.7127 316.	0.7043 316.	0.9091 320.	1.4259 332.	2.5167 356.	3.1032 369.	3.0540 367.	1.8334 340.
6	0.8017 318.	0.5820 313.	0.5719 313.	0.7546 317.	1.2330 327.	2.2764 350.	2.9422 365.	3.1170 369.	2.0196 344.
5	0.4576 310.	0.4198 309.	0.4500 310.	0.5940 313.	0.8919 320.	1.3445 330.	1.7624 339.	2.0927 346.	1.4536 332.
4	0.2962 307.	0.3051 307.	0.3491 308.	0.4554 310.	0.6349 314.	0.8700 319.	1.1394 325.	1.4309 332.	1.0289 323.
3	0.2340 305.	0.2455 305.	0.2852 306.	0.3704 308.	0.5067 311.	0.6807 315.	0.8811 319.	1.1025 324.	0.7922 317.
2	0.2402 305.	0.2309 305.	0.2574 306.	0.3387 307.	0.4901 311.	0.7047 316.	0.8858 320.	1.0144 322.	0.6971 315.
1	0.3273 307.	0.2455 305.	0.2513 306.	0.3366 307.	0.5435 312.	0.9769 322.	1.1914 326.	1.0764 324.	0.6790 315.
	1	2	3	4	5	6	7	8	9

Fig. B.2. (Contd) ANL Neg. No. 116-78-171

BWR TEST PROBLEM - COARSE MESH SOLUTION - TWO-STEP LEAKAGE

NORMALIZED ASSEMBLY POWERS AT T= 0.2000E 01

MEAN POWER DENSITY= 0.8154958E 03 AVERAGE FUEL TEMPERATURE= 0.867526E 03

9	0.4571 602.	0.4692 605.	0.5297 633.	0.6710 708.	0.8861 822.	1.0857 921.	1.0968 908.	0.0 300.	0.0 300.
8	0.7262 782.	0.6864 747.	0.7489 772.	0.9699 889.	1.3867 1113.	1.9490 1406.	2.2863 1546.	2.3494 1520.	0.0 300.
7	0.8138 840.	0.6099 698.	0.6204 690.	0.8289 800.	1.3495 1085.	2.4890 1701.	3.2922 2065.	3.6826 2119.	2.3757 1425.
6	0.6814 751.	0.5009 626.	0.5072 617.	0.6930 716.	1.1751 981.	2.2646 1570.	3.1352 1976.	3.7523 2156.	2.5771 1532.
5	0.3928 558.	0.3655 536.	0.4026 551.	0.5481 629.	0.8496 794.	1.3293 1050.	1.8344 1298.	2.3036 1509.	1.6626 1153.
4	0.2588 468.	0.2696 473.	0.3148 496.	0.4199 554.	0.5991 654.	0.8428 786.	1.1377 941.	1.4681 1113.	1.0794 890.
3	0.2082 435.	0.2198 441.	0.2580 462.	0.3388 508.	0.4686 584.	0.6375 681.	0.8379 794.	1.0649 921.	0.7764 749.
2	0.2169 440.	0.2084 434.	0.2326 447.	0.3061 492.	0.4425 575.	0.6368 695.	0.8049 796.	0.9312 869.	0.6476 693.
1	0.2976 493.	0.2225 443.	0.2267 444.	0.3018 491.	0.4843 606.	0.8685 849.	1.0601 968.	0.9623 903.	0.6130 682.
	1	2	3	4	5	6	7	8	9

Fig. B.2. (Contd) ANL Neg. No. 116-78-179

BWR TEST PROBLEM - COARSE MESH SOLUTION - TWO-STEP LEAKAGE

NORMALIZED ASSEMBLY POWERS AT T= 0.3000E 01

MEAN POWER DENSITY= 0.9703024E 02 AVERAGE FUEL TEMPERATURE= 0.112733E 04

9	0.4999 726.	0.5052 731.	0.5546 774.	0.6821 884.	0.8806 1051.	1.0638 1200.	1.0656 1189.	0.0 300.	0.0 300.
8	0.7947 979.	0.7395 932.	0.7831 971.	0.9825 1142.	1.3716 1472.	1.8993 1906.	2.2088 2131.	2.2601 2121.	0.0 300.
7	0.8926 1062.	0.6582 862.	0.6481 854.	0.8370 1017.	1.3289 1433.	2.4185 2339.	3.1717 2905.	3.5309 3058.	2.2775 2031.
6	0.7490 937.	0.5418 761.	0.5307 752.	0.7003 897.	1.1579 1284.	2.2017 2150.	3.0224 2777.	3.6005 3112.	2.4731 2190.
5	0.4327 665.	0.3965 635.	0.4235 658.	0.5579 773.	0.8436 1014.	1.3001 1391.	1.7785 1767.	2.2255 2097.	1.6064 1578.
4	0.2871 539.	0.2946 546.	0.3346 581.	0.4335 665.	0.6046 810.	0.8378 1004.	1.1211 1234.	1.4419 1490.	1.0601 1168.
3	0.2340 492.	0.2433 501.	0.2786 531.	0.3567 599.	0.4839 707.	0.6498 848.	0.8471 1012.	1.0728 1198.	0.7815 951.
2	0.2473 500.	0.2343 491.	0.2551 510.	0.3281 574.	0.4669 693.	0.6657 864.	0.8358 1008.	0.9628 1115.	0.6685 863.
1	0.3424 576.	0.2525 505.	0.2510 506.	0.3265 572.	0.5162 736.	0.9194 1081.	1.1165 1250.	1.0095 1159.	0.6421 844.
	1	2	3	4	5	6	7	8	9

Fig. B.2. (Contd) ANL Neg. No. 116-78-178

BWR TEST PROBLEM - COARSE MESH SOLUTION - FLAT LEAKAGE

NORMALIZED ASSEMBLY POWERS AT T= 0.0

MEAN POWER DENSITY= 0.1000000E-05 AVERAGE FUEL TEMPERATURE= 0.300000E 03

9	0.9054 300.	0.8587 300.	0.8245 300.	0.8588 300.	0.9475 300.	0.9893 300.	0.8570 300.	0.0 300.	0.0 300.
8	1.4610 300.	1.2687 300.	1.1613 300.	1.2202 300.	1.4410 300.	1.7065 300.	1.6581 300.	1.3627 300.	0.0 300.
7	1.6608 300.	1.1325 300.	0.9492 300.	1.0107 300.	1.3421 300.	2.0990 300.	2.2223 300.	1.6581 300.	0.8570 300.
6	1.3842 300.	0.9255 300.	0.7680 300.	0.8319 300.	1.1506 300.	1.8871 300.	2.0990 300.	1.7066 300.	0.9893 300.
5	0.7755 300.	0.6648 300.	0.6131 300.	0.6759 300.	0.8675 300.	1.1506 300.	1.3421 300.	1.4410 300.	0.9475 300.
4	0.4977 300.	0.4844 300.	0.4908 300.	0.5529 300.	0.6759 300.	0.8319 300.	1.0107 300.	1.2202 300.	0.8588 300.
3	0.4007 300.	0.4001 300.	0.4216 300.	0.4908 300.	0.6131 300.	0.7680 300.	0.9492 300.	1.1613 300.	0.8245 300.
2	0.4287 300.	0.3923 300.	0.4001 300.	0.4844 300.	0.6648 300.	0.9255 300.	1.1325 300.	1.2687 300.	0.8587 300.
1	0.6052 300.	0.4287 300.	0.4007 300.	0.4977 300.	0.7755 300.	1.3842 300.	1.6608 300.	1.4610 300.	0.9054 300.
	1	2	3	4	5	6	7	8	9

Fig. B.3. BWR Test Problem Results - Coarse Mesh Flat Leakage Solution ANL Neg. No. 116-78-175

BWR TEST PROBLEM - COARSE MESH SOLUTION - FLAT LEAKAGE

NORMALIZED ASSEMBLY POWERS AT T= 0.4000E 00

MEAN POWER DENSITY= 0.1402642E-05 AVERAGE FUEL TEMPERATURE= 0.300000E 03

9	0.8254 300.	0.7917 300.	0.7785 300.	0.8379 300.	0.9548 300.	1.0249 300.	0.9098 300.	0.0 300.	0.0 300.
8	1.3305 300.	1.1682 300.	1.0965 300.	1.1929 300.	1.4586 300.	1.7801 300.	1.7845 300.	1.5217 300.	0.0 300.
7	1.5110 300.	1.0416 300.	0.8967 300.	0.9909 300.	1.3659 300.	2.2023 300.	2.4198 300.	1.9406 300.	1.0435 300.
6	1.2592 300.	0.8509 300.	0.7255 300.	0.8160 300.	1.1717 300.	1.9800 300.	2.2841 300.	1.9893 300.	1.1880 300.
5	0.7061 300.	0.6118 300.	0.5784 300.	0.6597 300.	0.8753 300.	1.1941 300.	1.4312 300.	1.5757 300.	1.0505 300.
4	0.4531 300.	0.4455 300.	0.4608 300.	0.5332 300.	0.6684 300.	0.8396 300.	1.0365 300.	1.2632 300.	0.8941 300.
3	0.3636 300.	0.3663 300.	0.3924 300.	0.4655 300.	0.5907 300.	0.7484 300.	0.9329 300.	1.1471 300.	0.8172 300.
2	0.3868 300.	0.3568 300.	0.3690 300.	0.4530 300.	0.6273 300.	0.8776 300.	1.0786 300.	1.2132 300.	0.8236 300.
1	0.5442 300.	0.3880 300.	0.3675 300.	0.4621 300.	0.7252 300.	1.2984 300.	1.5617 300.	1.3775 300.	0.8557 300.
	1	2	3	4	5	6	7	8	9

Fig. B.3. (Contd) ANL Neg. No. 116-78-174

BWR TEST PROBLEM - COARSE MESH SOLUTION - FLAT LEAKAGE

NORMALIZED ASSEMBLY POWERS AT T= 0.8000E 00

MEAN POWER DENSITY= 0.3336835E-05 AVERAGE FUEL TEMPERATURE= 0.300000E 03

9	0.7106 300.	0.6954 300.	0.7124 300.	0.8076 300.	0.9649 300.	1.0756 300.	0.9854 300.	0.0 300.	0.0 300.
8	1.1431 300.	1.0239 300.	1.0033 300.	1.1535 300.	1.4834 300.	1.8849 300.	1.9656 300.	1.7499 300.	0.0 300.
7	1.2960 300.	0.9110 300.	0.8212 300.	0.9622 300.	1.3996 300.	2.3495 300.	2.7017 300.	2.3469 300.	1.3172 300.
6	1.0797 300.	0.7439 300.	0.6645 300.	0.7931 300.	1.2015 300.	2.1123 300.	2.5480 300.	2.3949 300.	1.4778 300.
5	0.6064 300.	0.5356 300.	0.5284 300.	0.6364 300.	0.8863 300.	1.2560 300.	1.5585 300.	1.7685 300.	1.1988 300.
4	0.3891 300.	0.3896 300.	0.4177 300.	0.5048 300.	0.6575 300.	0.8507 300.	1.0733 300.	1.3248 300.	0.9447 300.
3	0.3104 300.	0.3178 300.	0.3505 300.	0.4292 300.	0.5584 300.	0.7203 300.	0.9095 300.	1.1267 300.	0.8066 300.
2	0.3268 300.	0.3058 300.	0.3243 300.	0.4079 300.	0.5736 300.	0.8091 300.	1.0014 300.	1.1336 300.	0.7733 300.
1	0.4566 300.	0.3297 300.	0.3199 300.	0.4110 300.	0.6531 300.	1.1753 300.	1.4196 300.	1.2578 300.	0.7843 300.
	1	2	3	4	5	6	7	8	9

Fig. B.3. (Contd) ANL Neg. No. 116-78-166

BWR TEST PROBLEM - COARSE MESH SOLUTION - FLAT LEAKAGE

NORMALIZED ASSEMBLY POWERS AT T= 0.1200E 01

MEAN POWER DENSITY= 0.2747864E-02 AVERAGE FUEL TEMPERATURE= 0.300000E 03

9	0.5708 300.	0.5768 300.	0.6282 300.	0.7641 300.	0.9682 300.	1.1287 300.	1.0714 300.	0.0 300.	0.0 300.
8	0.9158 300.	0.8472 300.	0.8855 300.	1.0969 300.	1.5012 300.	1.9993 300.	2.1818 300.	2.0351 300.	0.0 300.
7	1.0355 300.	0.7520 300.	0.7267 300.	0.9211 300.	1.4303 300.	2.5146 300.	3.0459 300.	2.8830 300.	1.6903 300.
6	0.8628 300.	0.6141 300.	0.5888 300.	0.7610 300.	1.2303 300.	2.2629 300.	2.8730 300.	2.9319 300.	1.8719 300.
5	0.4867 300.	0.4438 300.	0.4670 300.	0.6054 300.	0.8953 300.	1.3272 300.	1.7151 300.	2.0141 300.	1.3906 300.
4	0.3129 300.	0.3226 300.	0.3653 300.	0.4690 300.	0.6418 300.	0.8616 300.	1.1164 300.	1.3987 300.	1.0060 300.
3	0.2476 300.	0.2601 300.	0.3000 300.	0.3845 300.	0.5176 300.	0.6836 300.	0.8775 300.	1.0971 300.	0.7898 300.
2	0.2563 300.	0.2455 300.	0.2708 300.	0.3529 300.	0.5066 300.	0.7221 300.	0.9022 300.	1.0301 300.	0.7069 300.
1	0.3537 300.	0.2610 300.	0.2630 300.	0.3487 300.	0.5632 300.	1.0191 300.	1.2379 300.	1.1041 300.	0.6919 300.
	1	2	3	4	5	6	7	8	9

Fig. B.3. (Contd) ANL Neg. No. 116-78-165

BWR TEST PROBLEM - COARSE MESH SOLUTION - FLAT LEAKAGE

NORMALIZED ASSEMBLY POWERS AT T= 0.1400E 01

MEAN POWER DENSITY= 0.5430645E 04 AVERAGE FUEL TEMPERATURE= 0.416997E 03

9	0.5478 362.	0.5553 364.	0.6083 370.	0.7452 387.	0.9516 412.	1.1199 432.	1.0764 427.	0.0 300.	0.0 300.
8	0.8777 400.	0.8144 393.	0.8563 399.	1.0684 425.	1.4740 474.	1.9847 535.	2.2021 561.	2.1028 548.	0.0 300.
7	0.9929 413.	0.7227 383.	0.7028 381.	0.8977 405.	1.4064 466.	2.5020 596.	3.0943 666.	3.0524 661.	1.8344 516.
6	0.8287 394.	0.5912 368.	0.5705 366.	0.7433 387.	1.2124 443.	2.2562 567.	2.9236 646.	3.1040 667.	2.0215 538.
5	0.4687 353.	0.4288 349.	0.4540 353.	0.5928 369.	0.8836 404.	1.3229 456.	1.7353 505.	2.0730 545.	1.4491 471.
4	0.3029 334.	0.3132 336.	0.3562 341.	0.4599 353.	0.6330 374.	0.8556 401.	1.1178 432.	1.4107 466.	1.0214 420.
3	0.2411 327.	0.2537 329.	0.2932 334.	0.3768 344.	0.5085 359.	0.6736 379.	0.8678 401.	1.0891 427.	0.7873 392.
2	0.2509 328.	0.2402 327.	0.2649 330.	0.3451 340.	0.4952 357.	0.7056 382.	0.8824 402.	1.0099 417.	0.6952 380.
1	0.3472 339.	0.2558 329.	0.2573 329.	0.3405 339.	0.5488 363.	0.9925 414.	1.2052 439.	1.0757 424.	0.6759 378.
	1	2	3	4	5	6	7	8	9

Fig. B.3. (Contd) ANL Neg. No. 116-78-160

BWR TEST PROBLEM - COARSE MESH SOLUTION - FLAT LEAKAGE

NORMALIZED ASSEMBLY POWERS AT T= 0.2000E 01

MEAN POWER DENSITY= 0.8253372E 03 AVERAGE FUEL TEMPERATURE= 0.890799E 03

9	0.4417 606.	0.4583 611.	0.5234 644.	0.6722 726.	0.8973 851.	1.1032 957.	1.1110 941.	0.0 300.	0.0 300.
8	0.7046 789.	0.6691 756.	0.7351 784.	0.9641 911.	1.3941 1153.	1.9700 1466.	2.3271 1620.	2.3960 1595.	0.0 300.
7	0.7970 854.	0.5932 705.	0.6050 697.	0.8147 814.	1.3421 1116.	2.5108 1775.	3.3493 2171.	3.7726 2236.	2.4335 1495.
6	0.6685 763.	0.4879 632.	0.4944 623.	0.6795 727.	1.1650 1005.	2.2767 1633.	3.1780 2070.	3.8305 2268.	2.6407 1610.
5	0.3823 563.	0.3580 541.	0.3963 558.	0.5434 641.	0.8470 814.	1.3268 1080.	1.8399 1342.	2.3244 1569.	1.6848 1199.
4	0.2512 471.	0.2650 477.	0.3121 503.	0.4186 564.	0.5968 667.	0.8345 801.	1.1263 961.	1.4565 1141.	1.0756 913.
3	0.2026 437.	0.2163 444.	0.2559 467.	0.3368 516.	0.4638 593.	0.6255 689.	0.8193 804.	1.0420 935.	0.7626 761.
2	0.2121 443.	0.2048 437.	0.2291 451.	0.3017 497.	0.4350 582.	0.6217 702.	0.7826 804.	0.9046 878.	0.6294 699.
1	0.2939 499.	0.2177 446.	0.2209 447.	0.2935 494.	0.4723 611.	0.8525 863.	1.0368 983.	0.9306 910.	0.5899 684.
	1	2	3	4	5	6	7	8	9

Fig. B.3. (Contd) ANL Neg. No. 116-78-159

BWR TEST PROBLEM - COARSE MESH SOLUTION - FLAT LEAKAGE

NORMALIZED ASSEMBLY POWERS AT T= 0.3000E 01

MEAN POWER DENSITY= 0.9817201E 02 AVERAGE FUEL TEMPERATURE= 0.115516E 04

9	0.4853	0.4953	0.5491	0.6836	0.8915	1.0803	1.0788	0.0	0.0
	728.	737.	786.	906.	1087.	1246.	1231.	300.	300.
8	0.7748	0.7237	0.7704	0.9772	1.3788	1.9188	2.2466	2.3032	0.0
	984.	940.	983.	1167.	1520.	1980.	2226.	2219.	300.
7	0.8783	0.6426	0.6334	0.8234	1.3218	2.4389	3.2246	3.6139	2.3307
	1075.	867.	861.	1030.	1468.	2430.	3041.	3215.	2127.
6	0.7380	0.5296	0.5185	0.6873	1.1481	2.2129	3.0618	3.6722	2.5318
	949.	766.	757.	907.	1310.	2226.	2896.	3261.	2296.
5	0.4228	0.3897	0.4177	0.5535	0.8413	1.2974	1.7831	2.2442	1.6268
	669.	640.	665.	786.	1037.	1427.	1821.	2174.	1637.
4	0.2795	0.2902	0.3324	0.4326	0.6026	0.8298	1.1100	1.4307	1.0565
	541.	550.	588.	677.	825.	1020.	1256.	1522.	1195.
3	0.2282	0.2399	0.2768	0.3551	0.4796	0.6384	0.8296	1.0516	0.7689
	494.	504.	538.	607.	717.	856.	1021.	1211.	963.
2	0.2425	0.2307	0.2518	0.3240	0.4602	0.6519	0.8153	0.9386	0.6519
	503.	494.	515.	579.	700.	870.	1014.	1121.	868.
1	0.3390	0.2476	0.2451	0.3184	0.5051	0.9060	1.0967	0.9806	0.6206
	582.	507.	508.	574.	740.	1095.	1265.	1162.	844.
	1	2	3	4	5	6	7	8	9

Fig. B.3. (Contd) ANL Neg. No. 116-78-173

Distribution for ANL-78-51

Internal:

P. B. Abramson
C. H. Adams
R. Avery
W. P. Barthold
C. L. Beck
J. C. Beitel
S. K. Bhattacharyya
L. L. Briggs
L. Burris
J. Cahalan
S. G. Carpenter
Y. I. Chang
D. W. Cissel
P. Collins
T. A. Daly
S. A. Davis
J. Deen
K. Derstine
D. R. Ferguson
B. R. T. Frost
P. L. Garner
E. M. Gelbard
G. H. Golden
G. Grasseschi
H. Henryson
R. P. Hosteny
H. H. Hummel
R. N. Hwang
Kalimullah
E. U. Khan
M. J. King
J. H. Kittel
H. Komoriya
A. B. Krisciunas
J. A. Kyger
P. S. K. Lam
R. Lell
L. G. LeSage
M. J. Lineberry
D. Malloy
J. E. Matos
R. D. McKnight
L. J. Milton
H. O. Monson
Y. Orechwa
G. Palmiotti
E. M. Pennington
P. J. Persiani
P. A. Pizzica
D. C. Rardin
B. Reynolds
R. R. Rudolph
R. W. Schaefer
R. A. Shober (20)
J. J. Sienicki
J. L. Snelgrove
C. G. Stenberg
W. J. Sturm
S. F. Su
R. J. Teunis
C. E. Till
B. J. Toppel
A. Travelli
R. Turski
A. J. Ulrich
D. C. Wade
R. Wei
W. Woodruff
R. S. Zeno
ANL Contract File
ANL Libraries (5)
TIS Files (6)

External:

DOE-TIC, for distribution per UC-79d (264)
Manager, Chicago Operations Office
Chief, Chicago Patent Group
Director, Reactor Programs Div., CH
Director, CH-INEL
Director, DOE-RRT (2)
President, Argonne Universities Association
Applied Physics Division Review Committee:
- P. W. Dickson, Jr., Westinghouse Electric Corp.
- R. L. Hellens, Combustion Engineering, Inc.
- W. B. Loewenstein, Electric Power Research Inst.
- R. F. Redmond, Ohio State U.
- R. Sher, Stanford U.
- D. B. Wehmeyer, Detroit Edison Co.
- S. A. Werner, U. Missouri